8-21-2024 2:00 PM

Host-Pathogen Co-evolution with Various Transmission Modes of Infection and Density-Dependent Dynamics

bita ghodsi,

Supervisor: Wild, Geoff, *The University of Western Ontario*
A thesis submitted in partial fulfillment of the requirements for the Master of Science degree in Applied Mathematics

Abstract

Pathogens can be transmitted both vertically (from the parent to the offspring) and horizontally. Here, I model the co-evolution of pathogens and their hosts allowing for vertical and horizontal transmission and density-dependent host population growth. My analysis uses evolutionary game theory. I use computational methods to find that increasing vertical transmission does not always result in more benign disease outcomes. Instead, it can lead to higher pathogen-induced mortality. Furthermore, more benign outcomes evolve more readily when horizontal transmission is more profitable for the pathogen, and overall virulence increases as horizontal transmission becomes more profitable. The results also indicate that vertical transmission, when associated with high virulence, can drive selection-driven extinction of the pathogen, which highlights the importance of considering both transmission modes in evolutionary studies.

Keywords: adaptive dynamics, parasite, infectious disease, evolutionary epidemiology

Summary for lay audience

My research focuses on the co-evolution of pathogens (agents causing disease) and their hosts (the organisms they infect), exploring how diseases spread and evolve. There are two main ways pathogens can transmit: from parent to offspring (vertical transmission) and between individuals in the same generation (horizontal transmission). Understanding these patterns helps us learn how diseases affect their hosts over time.

Using mathematical models and computer simulations, I study these interactions to predict changes. Surprisingly, increasing transmission from parent to offspring does not always make the disease less harmful. In fact, it can sometimes make it deadlier.

I also found that the severity of a disease can increase if spreading between individuals becomes more advantageous for the pathogen. Interestingly, highly deadly diseases that rely on both vertical and horizontal transmission can sometimes drive themselves to extinction by killing their hosts too quickly.

These findings help us understand the complex co-evolutionary relationships between hosts and pathogens, showing that the way diseases spread greatly influences their overall impact.

Co-Authorship statement

Chapter 2 will be submitted for publication co-authored by myself, Bita Ghodsi, and my supervisor, Geoff Wild (in that order). The order of authorship reflects the extent of the contribution made to the research. Wild and I jointly conceived of the research. I developed the model and the computational methods, I generated the results, and I drafted the chapter, all under Wild's guidance.

"If you think you are too small to make a difference, try sleeping with a mosquito."

– Dalai Lama

Acknowledgements

I would like to extend my heartfelt gratitude to those who have supported me throughout this journey.

First, I want to thank my big sister Ghazal for her unconditional love and support; my brother Reza for his constant motivation, for showing me the way, and sharing his invaluable experience; my brother Kiyan for always being a heartwarming presence and inspiration; and foremost, my parents for their unwavering and consistent support and love at all times.

I am also deeply grateful to my friends for their understanding, patience, and encouragement. Your companionship and support have been invaluable.

Lastly, I would like to express my sincere appreciation to my supervisor for their guidance, insight, and support throughout my research. Your expertise and encouragement have been instrumental in the completion of this thesis.

Thank you all for your unwavering support and belief in me.

Contents

List of Figures

List of Appendices

Chapter 1

Introduction

1.1 Host-Parasite Relationships

This thesis is about parasitism and the evolution of the relationship between parasites and their hosts. Parasitism is a widespread and ecologically significant interaction in which one organism, the parasite, lives on or within another living organism, the host. The parasite obtains nutrients of the host and causes some degree of real damage to it. Parasites include a diverse array of organisms such as bacteria, viruses, fungi, protozoa, helminths (worms), and arthropods . They can harm their hosts, causing anything from mild discomfort to severe illness or death (Price, 1980). Understanding parasitism is crucial for its implications in health, disease, and ecological balance, and evolutionary processes.

Hosts provide the necessary environment and resources for parasites to survive and reproduce. This relationship is inherently detrimental to the host, often resulting in reduced fitness, such as decreased health, reproductive success, or survival. The

interactions between hosts and parasites are complex, influencing the behavior and evolution of both parties involved (Price, 1980).

Studying the evolutionary dynamics of host-parasite interactions is essential for several reasons. Firstly, parasites play a significant role in regulating host populations and maintaining ecosystem balance (Britton, 2003). Secondly, the co-evolution of parasites and hosts drives evolutionary changes, providing insights into natural selection and adaptation (Abrams et al., 1993). Lastly, understanding these dynamics can help develop strategies to control parasitic diseases, which have substantial impacts on public health, agriculture, and economic stability (Godfray, 1994).

By modeling these interactions mathematically, this thesis aims to explore the ecological and evolutionary implications of parasitism. Mathematical models provide valuable insights into the dynamics of host-parasite systems, aiding in the development of strategies to manage parasitic diseases and maintain ecological balance. Tools such as invasion analysis and adaptive dynamics are particularly useful. Invasion analysis helps us understand how mutant traits can spread through a population, while adaptive dynamics offers a framework for studying the long-term evolution of these traits under ecological and evolutionary pressures. These approaches enable us to predict potential evolutionary outcomes and stability within host-parasite interactions (Dercole and Rinaldi, 2008).

1.2 Evolutionary Game Theory

Evolutionary Game Theory is a framework that applies the principles of game theory to evolutionary biology, providing insights into how strategic interactions among individuals influence evolutionary outcomes. Evolutionary Game Theory generally models the evolution of strategies in populations. Adaptive dynamics is a

theoretical framework that builds upon the principles of evolutionary game theory to bridge the fields of ecology and evolution. Adaptive dynamics focuses on the long-term evolutionary changes of continuous traits (Dercole and Rinaldi, 2008). It considers how interactions between individuals with different traits affect the process of selection. When mutations are very small, adaptive dynamics defines a fitness landscape and describes evolutionary changes using a system of ordinary differential equations. This approach models how new traits evolve and how traits with lower fitness are eliminated through extinction. The process involves the invasion and fixation of rare lineages: a new lineage appears and, if it successfully invades, it becomes fixed in the population before the next mutation occurs.

1.2.1 ESS and Convergence Stability for One Species

It is essential to introduce some fundamental concepts that support the analysis of evolutionary dynamics. Consider a population where all individuals are of type x^*. This value is considered an evolutionary equilibrium if the population can maintain this state without further changes occurring (Christiansen, 1991).

Two other important concepts in this regard are evolutionarily stable strategy (ESS) and convergence stability. Previous work of Maynard Smith and Price (1973) on ESS provided a framework for analyzing the stability and persistence of different strategies in competitive interactions. An ESS is a strategy that, if adopted by the majority of a population, cannot be invaded by any alternative strategy with higher reproductive fitness (Maynard Smith and Price, 1973; Eshel and Motro, 1981). Convergence stability refers to the ability of a population to return to a stable state after a small perturbation. In the context of my study, convergence stability measures the long-term behavior of the host-parasite system. Specifically, I am interested in investigating whether the system reaches a stable equilibrium and if the evolutionary

dynamics lead to convergence toward this equilibrium. This concept is also known as a continuously stable strategy (CSS) as described by Eshel (1983).

While an ESS ensures that natural selection will not drive a system away from the given state, it does not provide insights into how the system initially reaches that state. On the other hand, convergence stability focuses on how a particular state is achieved through the process of selection, ensuring the system returns to equilibrium after small perturbations.

By using these fundamental concepts into my analysis, I aim to uncover the evolutionary outcomes and convergence behavior of the host-parasite system. The invasion fitness function, represented by $W(x_m, x)$, denotes the rate at which a rare lineage, x_m, grows in a population dominated by a resident lineage, x (Metz et al., 1992; Dieckmann and Law, 1996). $W(x_m, x)$ is assumed to be twice continuously differentiable in both x and x_m. For x^* to be an evolutionary equilibrium, we have:

$$\left.\frac{\partial W}{\partial x_m}\right|_{x_m=x=x^*} = 0. \tag{1.2.1}$$

For x^* to be evolutionarily stable, we require the strict inequality $W(x_m, x^*) < W(x^*, x^*)$. Therefore, for any x^* that satisfies Condition (1.2.1), the following must hold for all $x_m \neq x^*$:

$$W(x_m, x^*) - W(x^*, x^*) \approx \frac{1}{2}\left.\frac{\partial^2 W}{\partial x_m^2}\right|_{x_m=x=x^*} (x_m - x^*)^2 \leq 0,$$

leading to $\left.\frac{\partial^2 W}{\partial x_m^2}\right|_{x_m=x=x^*} < 0$ as a sufficient condition for evolutionary stability, as

noted by Taylor (1996). Therefore, I summarize the sufficient ESS conditions by:

$$\begin{aligned} \left.\frac{\partial W}{\partial x_m}\right|_{x_m=x=x^*} &= 0, \\ \left.\frac{\partial^2 W}{\partial {x_m}^2}\right|_{x_m=x=x^*} &< 0. \end{aligned} \tag{1.2.2}$$

Inspired by Christiansen (1991), the evolutionary equilibrium x^*, satisfying Condition (1.2.1), is convergence stable if for any x close to x^*, a variant x_m near x has a positive fitness increment when the distance between x_m and x^* is less than that between x and x^*. This can be represented by:

$$W(x_m, x) > W(x, x) \Leftrightarrow |x - x^*| > |x_m - x^*|. \tag{1.2.3}$$

From Condition (1.2.3), holding $|x - x^*| > |x_m - x^*|$ true, we obtain:

$$W(x_m, x) - W(x, x) \approx \left.\frac{\partial W}{\partial x_m}\right|_{x_m=x} (x_m - x) > 0,$$

which can be represented by:

$$\begin{cases} \text{if} \quad x < x^* \quad \text{then} \quad \left.\dfrac{\partial W}{\partial x_m}\right|_{x_m=x} > 0, \\ \text{if} \quad x^* < x \quad \text{then} \quad \left.\dfrac{\partial W}{\partial x_m}\right|_{x_m=x} < 0. \end{cases} \tag{1.2.4}$$

It follows that the condition $\dfrac{d}{dx}\left(\left.\dfrac{\partial W}{\partial x_m}\right|_{x_m=x}\right)_{x=x^*} \leq 0$ must hold in addition to 1.2.1. Therefore, I summarize the sufficient convergence stability conditions by:

$$\begin{aligned} \left.\frac{\partial W}{\partial x_m}\right|_{x_m=x=x^*} &= 0, \\ \left.\frac{\partial^2 W}{\partial x_m^2} + \frac{\partial^2 W}{\partial x \partial x_m}\right|_{x_m=x=x^*} &< 0. \end{aligned} \tag{1.2.5}$$

System (1.2.5) ensures that after a small perturbation from the evolutionary equilibrium, x^*, population will naturally return to it over time.

We can model evolution as a process of successive invasion-displacement events, where a beneficial mutant appears and replaces the resident population before a new mutant can emerge (Metz et al., 1992). The evolution of a trait over evolutionary time τ is driven by the fitness gradient of the mutant trait evaluated at the resident trait, and is proportional to this gradient. This can be mathematically expressed as:

$$\frac{dx}{d\tau} = k \frac{\partial W}{\partial x_m}\bigg|_{x_m = x}, \tag{1.2.6}$$

where k is a non-negative constant that scales the rate of evolutionary change (Dieckmann and Law, 1996). The partial derivative in Equation (1.2.6) implies that the differences between the mutant and resident traits are very small, indicating weak selection. The trait expression x^* is defined as an evolutionary equilibrium if it satisfies Equation (1.2.1), making it a solution to Equation (1.2.6). Additionally, meeting the strict convergence stability conditions ensures that x^* is a locally asymptotically stable solution to Equation (1.2.6). I later extend these dynamics to two dimensions (two traits), considering them as co-evolution.

1.2.2 Example: Evolution of Body Size in a Predator

To illustrate the concepts of evolutionarily stable strategy and convergence stability, I consider a simple one-species example that can be found in Abrams et al. (1993). Let's examine a species where body size is an evolutionary trait that affects the fitness of an individual. The fitness function of an individual with body size of x_m

in a resident population with mean trait value of x, where x_m is near x, is given by:

$$W(x_m, x) = f\left(\frac{x_m}{x}\right) - d(x_m), \tag{1.2.7}$$

where $f(\frac{x_m}{x})$ denotes the probability of winning contests multiplied by the benefit from winning contests, which is an increasing function of $\frac{x_m}{x}$, and $d(x)$ represents the cost of the trait. For x^* to be convergence stable, it must meet Condition (1.2.5). Thus, we have:

$$\begin{aligned} \left.\frac{\partial W}{\partial x_m}\right|_{x_m=x=x^*} &= \frac{1}{x^*} f'(1) - d'(x^*) = 0, \\ \frac{d}{dx}\left[\left.\frac{\partial W}{\partial x_m}\right|_{x_m=x}\right]_{x=x^*} &= -\frac{1}{x^{*2}} f'(1) - d''(x^*) < 0, \end{aligned}$$

This condition holds if (but not only if) $d''(x) > 0$. For x^* to also be an ESS, it must satisfy Condition (1.2.2), resulting in:

$$\left.\frac{\partial^2 W}{\partial x_m^2}\right|_{x_m=x=x^*} = \frac{1}{x^{*2}} f''(1) - d''(x^*) < 0.$$

These are the general stability conditions for this fitness function. Notably, one stability definition does not necessarily imply the other. For example, for the Function (1.2.7), If $d(x_m) = 2x_m^2$ and $f\left(\frac{x_m}{x}\right) = \frac{1}{2}\left(\frac{x_m}{x}\right)^8$, then $x^* = 1$ is convergence stable but not an ESS.

1.2.3 Two-Species Co-evolution

In a two-species system, the evolutionary dynamics become more complex as each species' fitness depends not only on its own trait values but also on the trait values of the other species. For instance, Abrams et al. (1993) explains the co-evolution of predator-prey relationships, emphasizing that these interactions involve contin-

uous adaptation by both species. Predators and prey have selective pressures on each other, leading to evolutionary changes such as new defences in prey and more effective hunting strategies in predators. This process can result in an evolutionary arms race, where each species constantly evolves to surpass the other, or in stable co-evolutionary states where both species reach a balance in their adaptations.

In the context of two co-evolving species, the definition of an Evolutionarily Stable Strategy (ESS) extends to include the interactions between the species. For the first species with resident trait x and mutant trait x_m, and the second species with resident trait y and mutant trait y_m, the fitness of the mutant parasite and the mutant host are denoted by $W_p(x_m; x, y)$ and $W_h(y_m; x, y)$, respectively, representing the fitness of a mutant parasite and a mutant host when the (x, y) are resident traits. For a pair, (x^*, y^*), to be evolutionarily stable, the sufficient condition would be:

$$\begin{aligned} W_p(x^*; x^*, y^*) &> W_p(x_m; x^*, y^*) \text{ for all } x_m \neq x^* \\ W_h(y^*; x^*, y^*) &> W_h(y_m; x^*, y^*) \text{ for all } y_m \neq y^*, \end{aligned} \tag{1.2.8}$$

showing that neither species can increase its fitness by changing the trait value (Maynard Smith and Price, 1973).

We model co-evolution of the host-parasite by generalizing the dynamics of System (1.2.6) for a two-species system, resulting in

$$\begin{aligned} \frac{dx}{d\tau} &= k_p \frac{\partial W_p}{\partial x_m}\bigg|_{x_m=x} \\ \frac{dy}{d\tau} &= k_h \frac{\partial W_h}{\partial y_m}\bigg|_{y_m=y}, \end{aligned} \tag{1.2.9}$$

where k_p and k_h are non-negative constants which scale the rate of evolutionary change (Dieckmann and Law, 1996).

We can also evaluate convergence stability of System (1.2.9) to examine whether the population dynamics will evolve towards the ESS for both species over time. For the equilibrium (x^*, y^*) to be convergence stable, small perturbations in the traits should result in evolutionary dynamics that return the system to (x^*, y^*). For that, the real parts of the eigenvalues of the Jacobian matrix associated with linearization of System (1.2.9) at the equilibrium should be negative, ensuring the system returns to (x^*, y^*) after small perturbations.

1.3 Example of Co-evolution: Host-Parasitoid

Now, as an example of co-evolution, I will examine the co-evolutionary dynamics of a host-parasitoid system. In this section, I introduce parasitoids and analyze how the interactions between parasitoids and their hosts can drive evolutionary changes in both populations. This analysis will include modeling population dynamics, developing fitness functions, and exploring the stability states.

1.3.1 Parasitoids

Parasitoids are a unique group of parasites whose larvae feed exclusively on the bodies of other arthropods, ultimately leading to the host's death (Godfray, 1994). Unlike predators, parasitoids always kill their host and require only a single host to complete their development. They lay their eggs on or in the bodies of hosts, and the larvae feed on the host's tissues until pupation, by which time the host is generally dead (Godfray, 1994). This intimate interaction with their hosts is a key aspect of their role in evolutionary ecology.

1.3.2 Nicholson-Bailey and Population Dynamics

The earliest and simplest models for the behaviors of hosts and parasitoids were developed by Nicholson and Bailey (Nicholson and Bailey, 1935). First, we take a look at the Nicholson-Bailey model and its results and then see how Britton (2003) has modified the model.

The model of Nicholson and Bailey (1935) was developed to study oscillations in host-parasitoid systems. This model operates in discrete time, and while a continuous model will be analyzed later, the ideas and principles remain fundamentally the same. The census occurs at the beginning of each season, prior to any parasitism, and counts adult parasitoids as well as the stages of the host that are subject to parasitization. Let H_n and P_n represent the number of hosts and parasitoids, respectively, at the beginning of generation n. The population dynamics of this model are described as follows:

$$\begin{aligned} H_{n+1} &= R_0 H_n f(H_n, P_n), \\ P_{n+1} &= cH_n(1 - f(H_n, P_n)), \end{aligned} \tag{1.3.1}$$

where R_0 refers to the host basic reproductive ratio, i.e., the per capita production of the host per generation in the absence of parasitism, c indicates the average number of eggs laid per generation by an adult parasitoid in a single host that will survive to breed in the next generation, and $f(H_n, P_n)$ is the fraction of hosts not parasitized over one generation. So that after parasitism, the number of unparasitized hosts would be $H_n f(H_n, P_n)$ while the number of parasitized hosts would be $H_n(1 - f(H_n, P_n))$.

There are some key assumptions in their model. First, it assumes no density-

dependent effects on the host population, leading to exponential growth in the absence of parasitism (assuming $R_0 > 1$). Second, it assumes parasitoids can infect any host they encounter without limit. Finally, they model $f(H_n, P_n)$ by treating parasitoid search as a Poisson process with searching efficiency α. The search is continuous between census points: $\frac{dH_n}{dt} = -\alpha P_n H_n$ for $n < t < n + \tau$. The parasitoid number remains constant during the search. Thus, by the interval's end, $H(n + \tau) = H_n f(H_n, P_n) = H_n \exp(-aP_n)$, where $a = \alpha\tau$. Therefore, $f(H_n, P_n) = \exp(-aP_n)$. Thus, Equations (1.3.1) become:

$$\begin{aligned} H_{n+1} &= R_0 H_n \exp(-aP_n) \\ P_{n+1} &= cH_n(1 - \exp(-aP_n)). \end{aligned} \tag{1.3.2}$$

To find the host and parasitoid populations sizes at equilibrium, denoted as (H^*, P^*), we solve the equations $H_{n+1} = H_n$ and $P_{n+1} = P_n$. This yields:

$$\begin{aligned} P^* &= \frac{1}{a}\log(R_0), \\ H^* &= \frac{P^* R_0}{c(R_0 - 1)}. \end{aligned}$$

Now, I examine the stability of the equilibrium. I apply the Jury condition for the stability of discrete-time linear systems, which are:

$$\begin{aligned} |\text{trace} J^*| &< \det J^* + 1, \\ \det J^* &< 1, \end{aligned} \tag{1.3.3}$$

where J^* is the Jacobian matrix of the System (1.3.2) at equilibrium. However, for $R_0 > 1$, the determinant exceeds one, violating the second Jury condition. This suggests that the system has at least one eigenvalue which lies outside the unit

circle. Consequently, the Nicholson-Bailey model predicts unbounded oscillations in the host-parasitoid system, which does not reflect real-life dynamics. This issue is illustrated through numerical results in Figure (1.1). In this model, some unrealistic

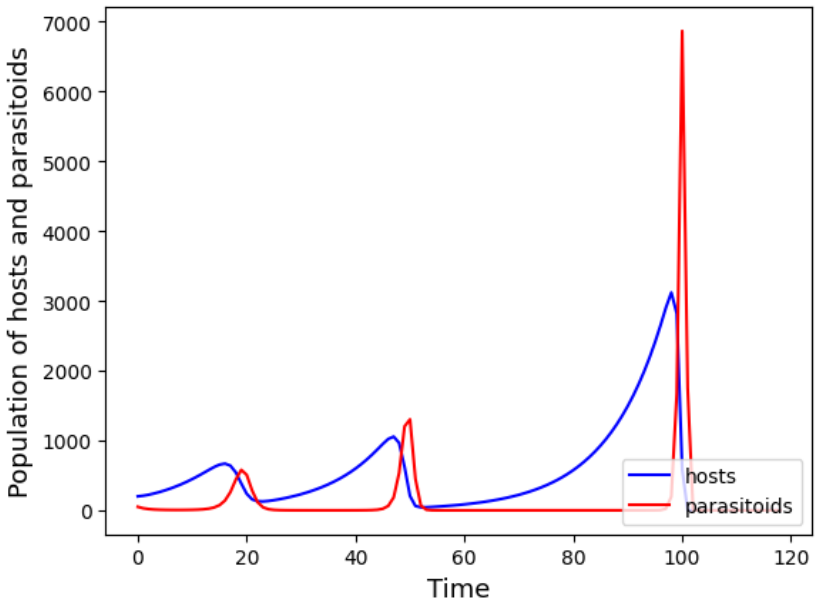

Figure 1.1: Numerical integration of the Nicholson-Bailey host-parasitoid model, assuming parasitoid search follows a Poisson process. The model fails as the parasitoid population drops to zero. Consequently, the trajectory forms an outward spiral, with peaks and troughs becoming more extreme until eventual extinction.

assumptions might have caused unrealistic results. Addressing each of them to adjust the model can result in a stable state. Britton (2003) suggested some potential modification in the clumped distribution of parasitoid search behavior that could be described by a negative binomial distribution, $\frac{dH_n}{dt} = -\alpha P_n H_n \left(1 + \frac{bP_n}{k}\right)^{-k}$ for $n < t < n + \tau$, which leads to:

$$f(H_n, P_n) = \left(1 + \frac{bP_n}{k}\right)^{-k},$$

where k is the clumping parameter. As k approaches infinity, $f(H_n, P_n)$ converges to

the exponential function e^{-bP_n}, thereby recovering the Poisson model. I present the numerical results of the modified Nicholson-Bailey model in Figure (1.2), demonstrating stability for a finite clumping parameter ($k = 1$).

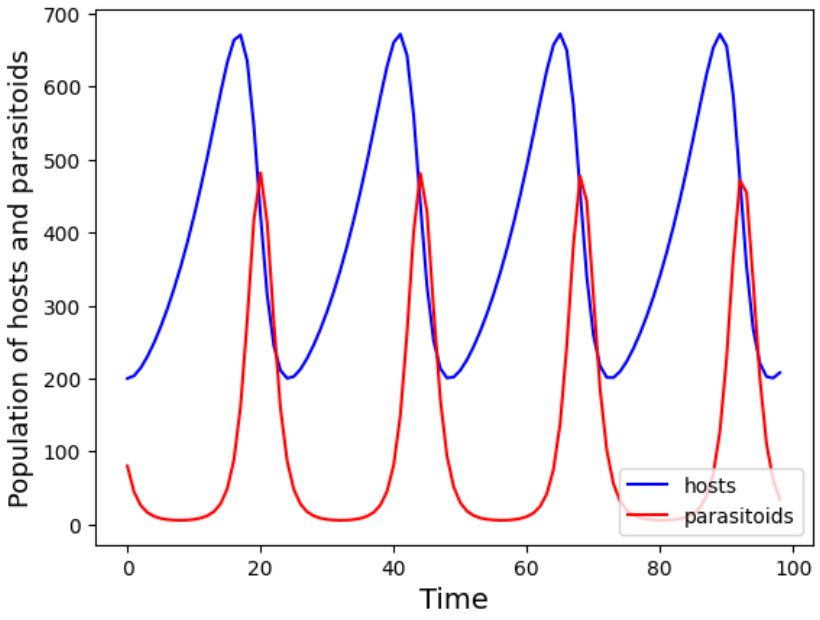

Figure 1.2: Numerical integration of the Nicholson-Bailey host-parasitoid model, assuming parasitoid search follows a binomial distribution when $k = 1$. The model demonstrates the interaction dynamics where the probability of finding a host is binomially distributed, affecting the population trajectories of both species. The result shows the fluctuations of the host and parasitoid populations over time.

1.3.3 Parasitoid Invasion

Now, I examine the adaptive dynamics and outcomes of the parasitoid-host system. Consider a host population susceptible to attack and infection by a resident parasitoid strain and a mutant parasitoid strain during a period of length τ. Let $\hat{P}_n$ denote the size of the mutant parasitoid population at the beginning of generation n. Assume that a and $\hat{a}$ are constant attack rates, and k is a constant reflecting the

extent to which the host population is clumped. c and $\hat{c}$ are the average numbers of eggs laid by an adult resident parasitoid and an adult mutant parasitoid, respectively, in a single host that will survive to the next generation. The dynamics of the two-parasitoid system are given by:

$$\begin{aligned} H_{n+1} &= R_0 H_n f(bP_n + \hat{b}\hat{P}_n), \\ P_{n+1} &= cH_n \frac{bP_n}{bP_n + \hat{b}\hat{P}_n}(1 - f(bP_n + \hat{b}\hat{P}_n)), \\ \hat{P}_{n+1} &= \hat{c}H_n \frac{\hat{b}\hat{P}_n}{bP_n + \hat{b}\hat{P}_n}(1 - f(bP_n + \hat{b}\hat{P}_n)), \end{aligned} \tag{1.3.4}$$

where $b = a\tau$, $\hat{b} = \hat{a}\tau$. This two-parasitoid system (System 1.3.4) has a mutant-free equilibrium $(H^*, P^*, 0)$.

The positive definiteness of the Jacobian matrix indicates local stability around an equilibrium point, meaning that small perturbations will converge back to the equilibrium. This stability property is related to the convergence behavior of the system. Now, I find the Jacobian matrix for the system at the mutant-free equilibrium to analyze the stability:

$$J_P^* = \begin{bmatrix} R_0 f(bP^*) & R_0 H^* f'(bP^*)b & -- \\ c(1 - f(bP^*)) & -cH^* f'(bP^*)b & -- \\ 0 & 0 & \frac{\hat{b}\hat{c}}{bc} \end{bmatrix}. \tag{1.3.5}$$

The elements marked $--$ are not of interest. The positive definiteness of the matrix depends only on the element in the lower right corner of this Jacobian matrix, which determines the invasion potential of the mutant parasitoid. I consider this element as the parasitoid fitness. I will model b and c as functions of a continuous resident trait, x. Therefore, I express b and c as $b = b(x)$ and $c = c(x)$, respectively. I assume

a trade-off between $b(x)$ and $c(x)$, meaning that x has opposite effects on $b(x)$ and $c(x)$. Let x_m denote the mutant trait, with $\hat{c} = c(x_m)$ and $\hat{b} = b(x_m)$. Consequently, the fitness of the mutant parasitoid, denoted $W_P(x_m; x, y)$, can be expressed as:

$$W_P(x_m; x, y) = \frac{b(x_m)c(x_m)}{b(x)c(x)} \tag{1.3.6}$$

If $W_P(x_m; x, y) > 1$, then the mutant invades, and if the inequality is reversed, the mutant is eliminated.

Evolutionarily stable x^* is understood as:

$$x^* = \arg\max b(x)c(x) \tag{1.3.7}$$

This analysis provides a framework for understanding the conditions under which a mutant parasitoid strain can invade.

1.3.4 Host Invasion

In this section, I will analyze the host invasion dynamics. I consider both a resident host and a mutant host, each susceptible to attack and infection by a parasitoid over a period of length τ. Let $\hat{H}_n$ denote the size of the mutant host population at the beginning of generation n. Let R_0 and $\hat{R}_0$ represent the per capita production per generation of the resident and mutant hosts, respectively, in the absence of parasitism. Hosts can modify their attack rates in response to the presence of

parasitoids. The dynamics of the two-host system are given by:

$$\begin{aligned} H_{n+1} &= R_0 H_n f(bP_n), \\ P_{n+1} &= cH_n(1 - f(bP_n)) + c\hat{H}_n(1 - f(\hat{b}P_n)), \\ \hat{H}_{n+1} &= \hat{R}_0 \hat{H}_n f(\hat{b}P_n)., \end{aligned} \tag{1.3.8}$$

where $b = a\tau$, $\hat{b} = \hat{a}\tau$. This two-host System (1.3.8) has a mutant-free equilibrium $(H^*, P^*, 0)$.

Similar to the pathogen invasion, I explore the positive definiteness of the Jacobian matrix of System (1.3.8) at equilibrium, which is:

$$J_H = \begin{bmatrix} R_0 f(bP^*) & R_0 H^* f'(bP^*)b & -- \\ c(1 - f(bP^*)) & -cH^* f'(bP^*)b & -- \\ 0 & 0 & \hat{R}_0 f(\hat{b}P_n^*) \end{bmatrix}, \tag{1.3.9}$$

where $--$ indicates elements that are not relevant to our analysis. The positive definiteness of the matrix depends only on the element in the lower right, which we take as host fitness. I will model b and R_0 as functions of the host continuous evolutionary trait, y. Thus, I express $b = b(y)$ and $R_0 = R_0(y)$ for the resident host, and $\hat{b} = b(y_m)$ and $\hat{R}_0 = R_0(y_m)$ for the mutant host. Consequently, the fitness of the mutant host, y_m, in a resident population is given by:

$$W_h(y_m; x, y) = R_0(y_m) f(\hat{b}P_n^*). \tag{1.3.10}$$

Substituting the population size of the parasitoid at equilibrium, we have:

$$W_h(y_m; x, y) = R_0(y_m)\left(1 + \frac{b(y_m)}{b(y)}(\sqrt[k]{R_0(y)} - 1)\right)^{-k}. \tag{1.3.11}$$

If $W_h(y_m; x, y) > 1$, the mutant host invades, leading to:

$$\frac{(R_0(y))^{\frac{1}{k}} - 1}{b(y)} < \frac{(R_0(y_m))^{\frac{1}{k}} - 1}{b(y_m)}. \tag{1.3.12}$$

Evolutionarily stable y^* is understood as:

$$y^* = \arg\max \frac{(R_0(y))^{\frac{1}{k}} - 1}{b(y)}. \tag{1.3.13}$$

This analysis provides a framework for understanding the conditions under which mutant host strains can invade and establish themselves in a population, contributing to our understanding of host-parasitoid evolutionary dynamics.

1.4 Looking ahead

While models like the Nicholson-Bailey host-parasitoid one provide a solid foundation, they have limitations. In the discussed host-parasitoid model, each species optimizes its fitness independently without considering the other's strategy. This contrasts with Shillcock et al. (2023) and my work in the next chapter. Shillcock et al. (2023) introduces a game between the host and the pathogen, where each species' fitness depends on the other's strategy, so the fitness of each species is maximized given the strategy of the other. I will go further by developing a more general and complicated game, exploring both interspecies and intraspecies interactions. This includes scenarios where a mutant arises, and its growth rate depends on not only its own strategy but also the resident populations' strategies. This broader approach will help me understand scenarios where pathogens interact with other pathogens and hosts with other hosts, providing a more complete view of co-evolution. Shillcock et al. (2023) also points out issues with handling ver-

tical transmission (transmission from parent to offspring), which adds complexity to evolutionary dynamics. Including factors like vertical transmission and density-dependent effects, the model I introduce aims for a more detailed understanding of pathogen evolution.

Chapter 2

Host-Pathogen Co-evolution with Vertical Transmission of Infections and Density-Dependent Dynamics

2.1 Introduction

Pathogens can be transmitted vertically from parent to offspring. In humans, for example, this can occur before birth, during birth, and after birth, with examples including hepatitis, HIV, and rubella (Arora et al., 2022). In mammals more broadly, the protozoan *Toxoplasma gondii* can be transmitted from mother to fetus during pregnancy (Montoya and Liesenfeld, 2004). In insects, the *Wolbachia* bacterium is passed from mother to offspring through the eggs (Werren, 1997). In plants, vertical transmission can happen through pollen and seeds (Pagán et al., 2022). Of course pathogens can also spread through more usual (horizontal) means.

Vertical transmission is often predicted to select against pathogens that inflict excessive harm on their hosts (Cressler et al., 2016; Frank, 1996; Lipsitch et al., 1996; Stearns and Medzhitov, 2015; Úbeda and Jansen, 2016; Ewald, 1994). A vertically transmitted pathogen that is too virulent limits the reproductive potential of its host and cuts itself off from a ready source of new infections. It is easy to show theoretically that, all else being equal, vertically transmitted pathogens should be less virulent than those transmitted exclusively through horizontal means (e.g. Stearns and Medzhitov, 2015; Úbeda and Jansen, 2016). All else may not be equal, though. In fact, recent theoretical work has shown that when hosts co-evolve with their pathogens, vertical transmission can lead to higher levels of host harm (Shillcock et al., 2023).

Although recent theoretical work shows that vertical transmission can bring co-evolving pathogens and hosts into greater conflict (Shillcock et al., 2023), this work is far from complete. In particular, it is based on a model in which pathogen-induced mortality is the sole factor regulating host-population growth. If pathogen-induced mortality is too low, or absent, then the size of the host population grows without bound and the modelling paradigm upon which the conclusions rest fails (Metz et al., 1992). The implication here is that recent work may struggle to find co-evolutionary outcomes involving benign pathogens and can say nothing about phenomena like selection-driven extinction of the pathogen that have been observed elsewhere (van Baalen, 1998). To fill this gap, we must revise current approaches by incorporating self-regulation of host population growth.

Our goal is to understand how vertical transmission impacts pathogen-host co-evolution when host population growth is regulated by factors in addition to pathogen-induced mortality. Specifically, we asked how host demography (birth rate, death

rate) and the ease with which infections are created horizontally (later, profitability of horizontal transmission) interact with vertical transmission to shape co-evolutionary outcomes when growth of the host population is density-dependent. Unlike previous work, we find self-regulation of host population growth can mean vertically transmitted pathogens are driven to extremely low densities by selection under certain circumstances.

2.2 Population Dynamics

We use a standard model for the dynamics of a host population in the presence of an infectious agent. Let $S = S(t)$ represent the number of individuals currently uninfected but susceptible to infection in the future. Immediately following infection, individuals enter the exposed phase of the disease: they are infected but not yet infectious. Let $E = E(t)$ represent the number of exposed hosts. Exposed individuals progress to the infectious phase. Let $I = I(t)$ be the number of infectious hosts characterized by the onset of infectiousness. Our immediate aim is to describe the changes in S, E, and I over time and to predict the long-term dynamic behavior of the system.

The number of individuals of each category varies due to death, birth, and disease progression. We use b_s to denote the per-capita birth rate of susceptible and exposed hosts, b_I to denote the per-capita birth rate of infectious hosts, and $\mu(N) = \mu_0 N$ to denote the per-capita background mortality rate of hosts, where μ_0 is a positive constant and $N = S + E + I$ is the total population size (we achieve self regulation of host population growth with density-dependent background mortality). Exposed hosts become infectious at a rate of δ. We assume the infection increases the per-capita mortality rate of infectious but not exposed individuals by the rate of α as

pathogen-induced mortality rate.

The number of individuals of each category also varies due to disease transmission and recovery. The infection is transmitted both horizontally and vertically. Hosts in the infectious stage have the capacity to horizontally transmit the pathogen to susceptible individuals, with some constant rate noted as $\beta > 0$ which characterizes the pathogen's horizontal transmissibility from I to uninfected host. The infectious hosts have the capability to transmit the infection to their newborn offspring. The parameter v denotes the probability at which the offspring of an infectious host is born with the infection. We assume that exposed hosts are incapable of transmitting the disease, either horizontally or vertically. Additionally, we assume that all infected newborn offspring are initially exposed and not infectious. Infectious hosts can recover from an infection. The infection is cleared from the infectious host at the recovery rate, γ. After clearance, the host is assumed to be immediately susceptible again.

For later use, we introduce a trade-off between the pathogen-induced mortality rate (α) and the horizontal transmission rate constant (β), as well as between the host recovery rate (γ) and b_I. The relationship between virulence and transmission (β) has been a subject of debate, with Alizon et al. (2009) noting that while the trade-off is controversial, it is widely recognized as a critical factor in pathogen evolution. Acevedo's meta-analysis (Acevedo et al., 2019) further supports this, demonstrating a generally positive relationship between virulence and β. Additionally, we consider a trade-off involving the host's energy budget, where any energy allocated to immune function (γ) reduces the energy available for reproduction, thereby influencing b_I. Consequently, we denote these relationships as $\beta = \beta(\alpha)$ and $b_I = b_I(\gamma)$

where $\beta^{'}(\alpha) > 0, \beta''(\alpha) < 0$, $b_I^{'}(\gamma) < 0$, and $b_I''(\gamma) < 0$. We specifically define

$$\begin{aligned} \beta(\alpha) &= k\alpha^n \\ b_I(\gamma) &= b_s - c\gamma^2, \end{aligned} \tag{2.2.1}$$

Here, n represents the profitability of the horizontal transmission, where $0 \leq n \leq 1$. This means that a one-percent increase in pathogen-induced mortality rate yields an n-percent increase in the horizontal transmission rate. The constants c and k act as scalars, adjusting the strength of the respective trade-offs. These trade-offs will become relevant when we develop fitness functions below.

We summarize our model assumptions with a system of differential equations:

$$\begin{aligned} \frac{dS}{dt} &= b_sS + b_sE + (1-v)b_I(\gamma)I - \beta(\alpha)IS + \gamma I - \mu(N)S \\ \frac{dE}{dt} &= \beta(\alpha)IS + vb_I(\gamma)I - \delta E - \mu(N)E \\ \frac{dI}{dt} &= \delta E - \gamma I - \alpha I - \mu(N)I. \end{aligned} \tag{2.2.2}$$

In the absence of the infection, the system of equations simplifies to

$$\begin{aligned} \frac{dS}{dt} &= (b_s - \mu(N))S \quad = (b_s - \mu_0 N)S = (b_s - \mu_0 S)S \\ \frac{dE}{dt} &= \frac{dI}{dt} = 0, \end{aligned} \tag{2.2.3}$$

which admits $(\frac{b_s}{\mu_0}, 0, 0)$ as the equilibrium solution (the disease-free equilibrium), suggesting that when there is no infection, the population is at equilibrium at $\bar{N}_o = \bar{S}_o = \frac{b_s}{\mu_0}$. In other words, in the absence of the disease, the host population size does not grow without bound as it has in previous models (Shillcock et al., 2023).

We test the local asymptotic stability of the disease-free equilibrium by investigat-

ing the eigenvalues of the Jacobian matrix,

$$J_{DFE} = \begin{bmatrix} -\mu(\bar{N}_0) & b_s & -\beta(\alpha)\bar{N}_0 + (1-v)b_I(\gamma) + \gamma \\ 0 & -\delta - \mu(\bar{N}_0) & \beta(\alpha)\bar{N}_0 + vb_I(\gamma) \\ 0 & \delta & -(\gamma + \alpha + \mu(\bar{N}_0)) \end{bmatrix}. \tag{2.2.4}$$

Specifically, the disease-free equilibrium is locally asymptotically stable whenever the real parts of all eigenvalues of J_{DFE} are negative. If one of the eigenvalues of this matrix has positive real part, then the disease-free equilibrium is unstable. We can immediately see that one of the eigenvalues is $-\mu(\bar{N}_0) < 0$. Given the block triangular structure of J_{DFE}, we conclude that the local asymptotic stability of the disease-free equilibrium hinges on the eigenvalues of the submatrix in the 2×2 block found in the lower right (the critical submatrix).

It is convenient to apply the Routh-Hurwitz criteria to the eigenvalues of the critical submatrix. The trace of the submatrix is negative, so the disease-free equilibrium loses its locally asymptotic stability if and only if the determinant of the submatrix is negative. In other words, the disease-free equilibrium is unstable when

$$(\delta + \mu(\bar{N}_0))(\gamma + \alpha + \mu(\bar{N}_0)) - \delta(\beta(\alpha)\bar{N}_0 + vb_I(\gamma)) < 0. \tag{2.2.5}$$

The previous line rearranges to

$$\frac{\delta}{(\delta + \mu(\bar{N}_0))} \frac{\beta(\alpha)\bar{N}_0 + vb_I(\gamma)}{(\gamma + \alpha + \mu(\bar{N}_0))} > 1. \tag{2.2.6}$$

The left-hand side of Condition (2.2.6) is known as the basic reproduction ratio, R_0. It gives the expected number of secondary infections generated by an exposed host in a fully susceptible population (van den Driessche and Watmough, 2002). In

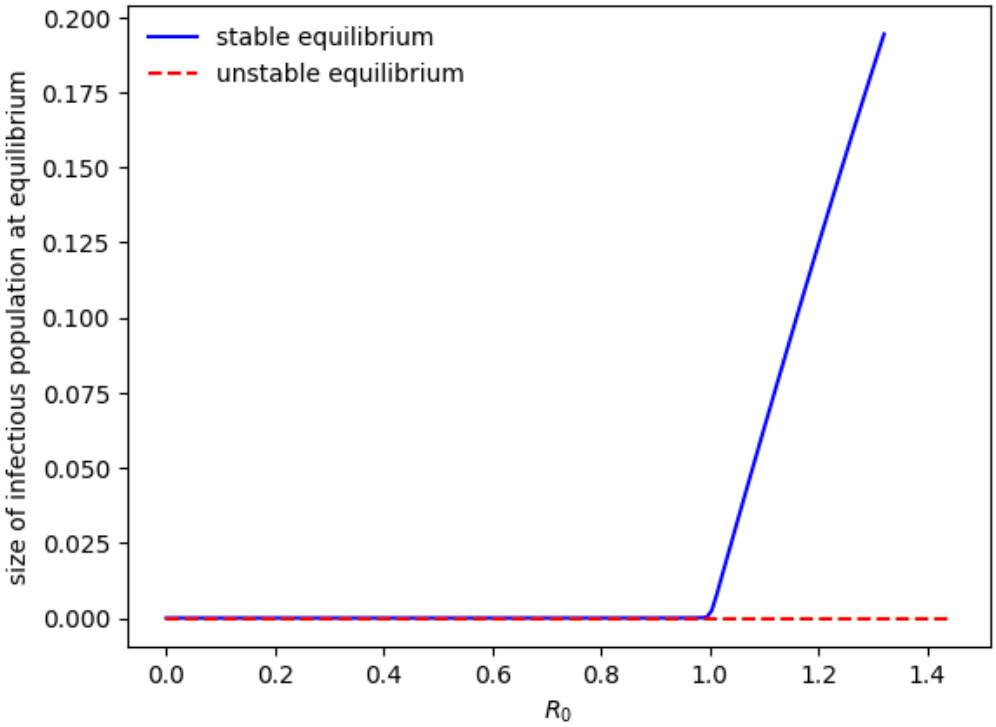

Figure 2.1: Population size of infectious hosts (I), plotted as a function of the basic reproduction number (R_0) for our model. We see a transcritical bifurcation at $R_0 = 1$ and stability is transferred from a disease-free equilibrium to an endemic equilibrium. This analysis is based on varying the rate at which exposed hosts become infectious, δ, within the range from 0.0 to 1.0. The model runs were performed with birth rate, $b_s = 0.2$, vertical transmission rate, $v = 0.4$, horizontal transmission profitability, $n = 0.4$, and background mortality rate, $\mu(N) = 0.15 \times N$, when N represents the total population.

Condition (2.2.6), $\frac{\delta}{(\delta+\mu(\bar{N}_0))}$ denotes the probability an exposed individual becomes infectious, $\frac{1}{(\gamma+\alpha+\mu(\bar{N}_0))}$ denotes the average duration an infectious individual remains in that state, and $\beta(\alpha)\bar{N}_0 + vb_I(\gamma)$ signifies the rate at which new infections are generated both horizontally and vertically. When $R_0 > 1$, the disease-free equilibrium typically loses its locally asymptotic stability, and an endemic equilibrium may exist. If such an equilibrium exists, exposed and infectious individuals occur in non-zero numbers, and this equilibrium can gain locally asymptotic stability. Numerical experiments support our expectations (Figure 2.1).

2.3 Fitness

To model the co-evolution of pathogen and host, we must determine the fitness of each. In this section, we describe the fitness of a rare pathogen lineage and that of a rare host lineage, at the endemic equilibrium represented by $\bar{S}$, $\bar{E}$, and $\bar{I}$. The same general approach appears many times in the literature (Abrams et al., 1993; Day and Burns, 2003; Shillcock et al., 2023).

2.3.1 Pathogen Fitness

We consider a rare mutant pathogen that induces a mortality rate of α_m on its host. This rare mutant is in a resident population dominated by a pathogen that induces mortality rate α at its endemic equilibrium. The following system represents the

population dynamics in the presence of both resident and mutant pathogen strains:

$$\begin{aligned}
\frac{dS}{dt} &= b_s S + b_s(E + E_m) + (1 - v)b_I(\gamma)(I + I_m) - \beta(\alpha)IS \\
&\quad - \beta(\alpha_m)I_m S + \gamma(I + I_m) - \mu(N)S \\
\frac{dE}{dt} &= \beta(\alpha)IS + vb_I(\gamma)I - \delta E - \mu(N)E \\
\frac{dI}{dt} &= \delta E - \gamma I - \alpha I - \mu(N)I \\
\frac{dE_m}{dt} &= \beta(\alpha_m)I_m S + vb_I(\gamma)I_m - \delta E_m - \mu(N)E_m \\
\frac{dI_m}{dt} &= \delta E_m - \gamma I_m - \alpha_m I_m - \mu(N)I_m.
\end{aligned} \tag{2.3.1}$$

Here, E_m and I_m denote the number of exposed and infectious hosts, respectively, carrying the mutant pathogen, N denotes the total population of residents and mutants, and we assume that no host can be infected by more than one strain of pathogen. Linearizing this model at the mutant-free equilibrium, where no mutant individual is present, denoted by $(\bar{S}, \bar{E}, \bar{I}, 0, 0)$, results in a decoupled 5×5 matrix, with a 2×2 block decoupled in the lower right corner. This structure allows the growth of the rare mutant pathogen to be approximated using

$$\begin{bmatrix} \frac{dE_m}{dt} \\ \frac{dI_m}{dt} \end{bmatrix} = J_p \begin{bmatrix} E_m \\ I_m \end{bmatrix}, \tag{2.3.2}$$

where

$$J_p = \begin{bmatrix} -(\delta + \mu(\bar{N})) & \beta(\alpha_m)\bar{S} + vb_I(\gamma) \\ \delta & -(\gamma + \mu(\bar{N}) + \alpha_m) \end{bmatrix}, \tag{2.3.3}$$

and $\bar{N}$ represents the total population at the mutant-free equilibrium.

We can now apply the next-generation theorem to develop a mathematical expression of the pathogen invasion fitness (Hurford et al., 2009). We decompose J_p as

$F_p - V_p$, where

$$F_p = \begin{bmatrix} 0 & \beta(\alpha_m)\bar{S} + vb_I(\gamma) \\ 0 & 0 \end{bmatrix} \tag{2.3.4}$$

and

$$V_p = \begin{bmatrix} \delta + \mu(\bar{N}) & 0 \\ -\delta & \gamma + \alpha_m + \mu(\bar{N}) \end{bmatrix}. \tag{2.3.5}$$

We index the rows and columns of F_p and V_p as $i, j, k = 1, 2$, where category 1 refers to exposed hosts and category 2 refers to infectious hosts. That said, the ijth entry of F_p gives the rate at which a category j infection produces a new category i infection. When we invert the matrix V_p, we find

$$V_p^{-1} = \frac{1}{(\delta + \mu(\bar{N}))(\gamma + \mu(\bar{N}) + \alpha_m)} \begin{bmatrix} \gamma + \mu(\bar{N}) + \alpha_m & 0 \\ \delta & \delta + \mu(\bar{N}) \end{bmatrix}. \tag{2.3.6}$$

The jkth entry of V_p^{-1} is the average length of time a current category k infection spends as a category j infection during its lifetime. Having this decomposition, the ikth element of the matrix, $K_p = F_p V_p^{-1}$, is interpreted as the expected lifetime number of new type i infections produced by a given infection that is currently of type k. We call K_p the 'next generation matrix' for this reason.

The spectral radius of the next-generation matrix gives us the invasion fitness of the mutant pathogen within a resident pathogen population, denoted $W_p(\alpha_m; \alpha, \gamma)$. Given that K_p is a triangular matrix, its largest eigenvalue can easily be found, and doing so yields

$$W_p(\alpha_m; \alpha, \gamma) = \frac{\delta}{(\delta + \mu(\bar{N}))} \frac{\beta(\alpha_m)\bar{S} + vb_I(\gamma)}{(\gamma + \mu(\bar{N}) + \alpha_m)}, \tag{2.3.7}$$

where $\bar{S}$ and $\bar{N}$ are functions of α and γ. The mutant pathogen invades if $W_p(\alpha_m; \alpha, \gamma) >$

$W_p(\alpha;\alpha,\gamma) = 1$ and if the inequality is reversed, the mutant is eliminated. Provided selection is weak (and provided an additional, minor technical condition is met), a mutant pathogen that invades, eventually displaces the resident pathogen strain (Dercole and Rinaldi, 2008).

2.3.2 Host Fitness

We now consider a scenario where a rare lineage of mutant hosts has arisen within a resident population at its endemic equilibrium. These mutant hosts recover from infections at a rate of γ_m, compared to the resident hosts who recover at a rate of γ. The following system represents the population dynamics in the presence of both resident and mutant hosts:

$$\begin{aligned}
\frac{dS}{dt} &= b_s S + b_s E + (1-v)b_I(\gamma)I - \beta(\alpha)(I+I^m)S + \gamma I - \mu(N)S \\
\frac{dE}{dt} &= \beta(\alpha)(I+I^m)S + vb_I(\gamma)I - \delta E - \mu(N)E \\
\frac{dI}{dt} &= \delta E - \gamma I - \alpha I - \mu(N)I \\
\frac{dS^m}{dt} &= b_s S^m + b_s E^m + (1-v)b_I(\gamma_m)I^m - \beta(\alpha)(I+I^m)S^m + \gamma_m I^m \\
&\quad - \mu(N)S^m \\
\frac{dE^m}{dt} &= \beta(\alpha)(I+I^m)S^m + vb_I(\gamma_m)I^m - \delta E^m - \mu(N)E^m \\
\frac{dI^m}{dt} &= \delta E^m - \gamma_m I^m - \alpha I^m - \mu(N)I^m.
\end{aligned} \tag{2.3.8}$$

Here, E^m and I^m denote the number of exposed and infectious hosts, respectively, carrying the mutant pathogen, S^m denotes the number of susceptible hosts to the mutant pathogen, and N represents the total population of residents and mutants. Linearizing this model around the mutant-free equilibrium, where no mutant individual is present, denoted by $(\bar{S}, \bar{E}, \bar{I}, 0, 0, 0)$, results in a decoupled 6×6 matrix,

with a decoupled 3×3 block in the lower right corner. This structure allows the growth of the rare mutant host to be approximated using

$$\begin{bmatrix} \frac{dS^m}{dt} \\ \frac{dE^m}{dt} \\ \frac{dI^m}{dt} \end{bmatrix} = J_h \begin{bmatrix} S^m \\ E^m \\ I^m \end{bmatrix}, \tag{2.3.9}$$

where

$$J_h = \begin{bmatrix} b_s - \beta(\alpha)\bar{I} - \mu(\bar{N}) & b_s & (1-v)b_I(\gamma_m) + \gamma_m \\ \beta(\alpha)\bar{I} & -\delta - \mu(\bar{N}) & vb_I(\gamma_m) \\ 0 & \delta & -(\gamma_m + \alpha + \mu(\bar{N})) \end{bmatrix}. \tag{2.3.10}$$

We decompose J_h as $F_h - V_h$, where

$$F_h = \begin{bmatrix} b_s & b_s & (1-v)b_I(\gamma_m) \\ 0 & 0 & vb_I(\gamma_m) \\ 0 & 0 & 0 \end{bmatrix} \tag{2.3.11}$$

and

$$V_h = \begin{bmatrix} \beta(\alpha)\bar{I} + \mu(\bar{N}) & 0 & -\gamma_m \\ -\beta(\alpha)\bar{I} & \delta + \mu(\bar{N}) & 0 \\ 0 & -\delta & \gamma_m + \alpha + \mu(\bar{N}) \end{bmatrix}. \tag{2.3.12}$$

The matrix F_h captures mutant host reproductive rates, and the inverse of V_h captures the expected amount of time a host remains in a given state (Hurford et al., 2009). The next generation matrix for the host is $K_h = F_h V_h^{-1}$, and its spectral-radius gives us the host invasion fitness, $W_h(\gamma_m; \alpha, \gamma)$. The matrix K_h is block triangular and its largest eigenvalues is also an eigenvalue of the 2×2 submatrix in the upper

left. It follows that

$$W_h(\gamma_m;\alpha,\gamma) = \frac{(K_{h_{11}} + K_{h_{22}}) + \sqrt{(K_{h_{11}} + K_{h_{22}}) - 4(K_{h_{11}}K_{h_{22}} - K_{h_{21}}K_{h_{12}})}}{2}, \quad (2.3.13)$$

where $K_{h_{ij}}$ denotes the element at row i and column j of K_h. The mutant host invades when $W_h(\gamma_m;\alpha,\gamma) > W_h(\gamma;\alpha,\gamma) = 1$, and if the inequality is reversed, the mutant is eliminated. Again, provided selection is weak (and provided an additional, minor technical condition is met), a mutant host that invades, displaces the resident host strain (Dercole and Rinaldi, 2008).

2.4 Evolutionary Dynamics

We model co-evolution as a series of invasion-displacement events: an advantageous mutant (either pathogen or host) arises and displaces the existing resident before another mutant (either pathogen or host) can arise (Metz et al., 1992). The rate of change of a trait expression over time τ is proportional to the fitness gradient of the mutant traits evaluated at the resident trait value. This allows us to describe the trajectories of pathogen-induced mortality and host recovery over evolutionary time τ as

$$\begin{aligned} \frac{d\alpha}{d\tau} &= k_p \frac{\partial W_p}{\partial \alpha_m}(\alpha;\alpha,\gamma) \\ \frac{d\gamma}{d\tau} &= k_h \frac{\partial W_h}{\partial \gamma_m}(\gamma;\alpha,\gamma), \end{aligned} \quad (2.4.1)$$

where k_p and k_h are constants that scale the rate of evolutionary change (Dieckmann and Law, 1996). The partial derivatives in Equation (2.4.1) indicate the difference between the mutant and resident traits is only very small; in other words, selection is weak. Equation (2.4.1) implies that mutant hosts and mutant pathogens do no co-occur. Thus, correlations between pathogen and host cannot emerge in this model.

A pair of host and pathogen traits, (α^*, γ^*), are at co-evolutionary equilibrium when they satisfy

$$\begin{aligned} \frac{\partial W_p}{\partial \alpha_m}(\alpha^*; \alpha^*, \gamma^*) &= 0 \\ \frac{\partial W_h}{\partial \gamma_m}(\gamma^*; \alpha^*, \gamma^*) &= 0. \end{aligned} \tag{2.4.2}$$

In other words, the pair (α^*, γ^*) is an equilibrium solution to Equation (2.4.1). That said, we consider a pair of traits at co-evolutionary equilibrium to be convergence stable if they are asymptotically stable under the dynamics described by Equation (2.4.1).

In general, convergence stable pairs like (α^*, γ^*) may still be susceptible to invasion by mutants (Geritz et al., 1998), that is they may lack evolutionary stability (Maynard Smith, 1982). To guarantee that (α^*, γ^*) are evolutionarily stable, we would like to require

$$\begin{aligned} W_p(\alpha_m; \alpha^*, \gamma^*) < W_p(\alpha^*; \alpha^*, \gamma^*) = 1 \\ W_h(\gamma_m; \alpha^*, \gamma^*) < W_h(\gamma^*; \alpha^*, \gamma^*) = 1 \end{aligned} \tag{2.4.3}$$

for all $\alpha_m \neq \alpha^*$ and $\gamma_m \neq \gamma^*$. However, we can only impose a local version of Condition (2.4.3). For α_m near α^* and γ_m near γ^*, we have

$$\begin{aligned} W_p(\alpha_m; \alpha^*, \gamma^*) &\approx 1 + \frac{1}{2}(\alpha_m - \alpha^*)^2 \frac{\partial^2 W_p}{\partial \alpha_m^2}(\alpha^*; \alpha^*, \gamma^*) \\ W_h(\gamma_m; \alpha^*, \gamma^*) &\approx 1 + \frac{1}{2}(\gamma_m - \gamma^*)^2 \frac{\partial^2 W_h}{\partial \gamma_m^2}(\gamma^*; \alpha^*, \gamma^*), \end{aligned} \tag{2.4.4}$$

where we have applied the definition of a co-evolutionary equilibrium to simplify

the previous line. It follows that,

$$\begin{aligned} \frac{\partial^2 W_p}{\partial \alpha_m^2}(\alpha^*; \alpha^*, \gamma^*) < 0 \\ \frac{\partial^2 W_h}{\partial \gamma_m^2}(\gamma^*; \alpha^*, \gamma^*) < 0 \end{aligned} \tag{2.4.5}$$

gives us a local condition for the evolutionary stability of (α^*, γ^*).

2.5 Numerical Analysis

We identify convergence stable pairs, numerically, in four steps. First, we guess values for (α^*, γ^*). Second, we find the endemic equilibrium corresponding to our guess by iterating Equation (2.2.2) forward in time. Third, we use the endemic equilibrium to calculate the fitness; specifically we calculate finite difference approximations for the partial derivatives for Equation (2.4.1). Fourth, we update the guess by adding some multiple of the appropriate partial derivative to the current values of α^* and γ^*, respectively. We repeat steps two to four until the absolute values of the finite difference approximations to the fitness derivatives in Equation (2.4.1) become sufficiently close to zero. To ensure the pair (α^*, γ^*) is also evolutionarily stable, we verify Condition (2.4.3) using finite difference approximations. The entire methodology is detailed in the appended Jupyter Notebook B.

2.6 Results

Before we detail the results, it is useful to make three fundamental observations. First, an increase in the birth rate, b_s, prompts a compensatory rise in the background mortality rate, $\mu(\bar{N})$, at equilibrium (Figure 2.2). Consequently, a rise in b_s triggers a reduction in the expected duration of infection and the expected life

span of the host. Second, as n increases, horizontal transmission becomes more profitable and therefore more attractive for the pathogen. From the host's perspective, increased n leads to greater risk of pathogen-induced mortality, as pathogen-induced mortality is associated with horizontal transmission. Third, a higher vertical transmission rate, ν, means a larger proportion of offspring from infected individuals being infected. From the host's perspective, infected offspring are costly, because they are of lower quality; however, infected offspring are beneficial to the pathogen as it does not need to impose pathogen-induced mortality in order to create these new infections. These points facilitate a clearer understanding of the results.

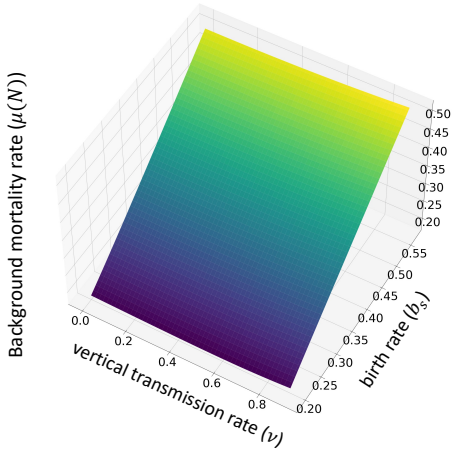

Figure 2.2: Variation of the background mortality rate when the population is at endemic and co-evolutionary equilibrium. We assume the rate of exposed hosts becoming infectious, $\delta = 1$, horizontal transmission profitability, $n = 0.27$, and the background mortality rate, $\mu(N) = 0.15 \times N$, when N represents the total population.

The results themselves, can be organized around the profitability of horizontal transmission, n. Generally, lower n leads to lower levels of trait expressions (i.e., smaller α^* and γ^*). By contrast, higher n leads to higher levels of trait expressions. How-

ever, within this generic framework, additional patterns emerge.

2.6.1 Lower Profitability of Horizontal Transmission Rate

We make two sets of observations for cases in which the profitability of horizontal transmission, represented by n, is low. The first set of observations concerns the effect of model parameters on the stable pathogen-induced mortality rate, α^*. The second set of observations concerns the effect of model parameters on the stable host recovery rate, γ^*.

Modifying the vertical transmission, v, and birth rate, b_s, influences the value of α^*. We observe that a rise in birth rate, b_s, elevates the pathogen-induced mortality rate α^* (Figure 2.3). A higher birth rate results in higher background mortality, as explained above, and in turn shortens the expected duration of infection. To maintain its reproductive success then, the pathogen must create new infections at a higher rate, and this need is reflected in the increased α^*, which improves horizontal transmission. With b_s held constant, an increase in v reduces the pathogen-induced mortality rate, α^* (Figure 2.3). As opportunities for vertical transmission become more frequent, the pathogen can maintain its reproductive success with less horizontal transmission which translates to lower α^*.

Adjusting the parameters of vertical transmission, v, and birth rate, b_s, impacts stable recovery rate, γ^*, as well.

When v is fixed at a low value, increasing b_s lowers recovery rate, γ^* (Figure 2.3). As mentioned above, larger reproductive rates are compensated by higher background mortality rate, which leads to a shorter host life span. Because of the trade-off involving birth rate when infected, the lower recovery rate allows the host to maintain its lifetime reproductive success in a shorter period of time. Notably, the

reduction in γ^* here is accompanied by an increase in α^* (Figure 2.3). This is explained by the lower value of n. Recall that when n is small, the risk associated with infection is low. Thus, the host is less concerned by the threat of the disease and more concerned with reduction in fitness connected to the density of its own population. Given v is low, the host is similarly less concerned by the risks of producing low-quality infected offspring.

Conversely, when v is fixed at a high value, an increase in b_s boosts γ^* (Figure 2.3). Now, an infected host prioritizes recovery because otherwise, it will transmit its infection to a significant fraction of its offspring. In other words, there is a shift toward enhancing the quality of reproductive output within a shortened life expectancy rather than the quantity.

When v is increased, with b_s held constant, we observe a reduction in recovery rate γ^* (Figure 2.3). This is interpreted as a response to the reduction in pathogen-induced mortality, α^*, that is in turn driven by greater opportunities for vertical transmission.

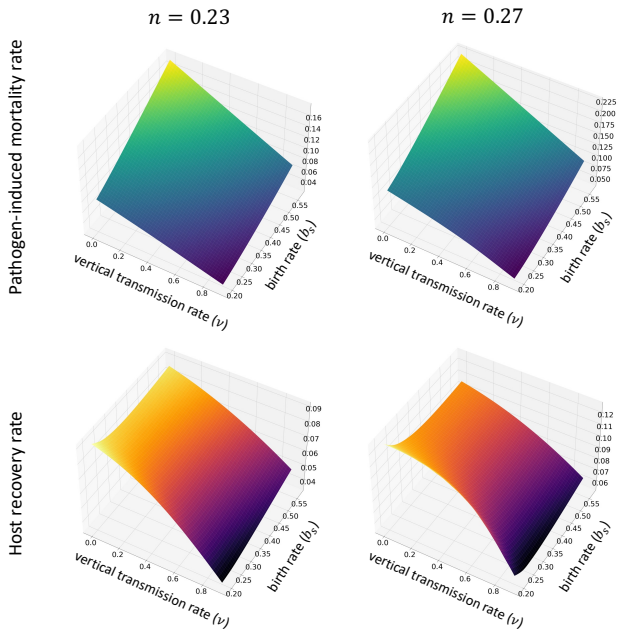

Figure 2.3: Variation in the evolutionarily stable values of pathogen-induced mortality rate (α^*) and host recovery rate (γ^*) across different levels of vertical transmission rates (v) and birth rates (b_s), at lower horizontal transmission profitability (n), specifically for $n = 0.23$ and $n = 0.27$. The first row of subplots details how α^* adapts to shifts in vertical transmission and birth rates for these lower n values, while the second row focuses on γ^*. We assume the rate of exposed hosts becoming infectious, $\delta = 1$, and the background mortality rate, $\mu(N) = 0.15 \times N$, when N represents the total population.

2.6.2 Higher Profitability of Horizontal Transmission Rate

We now consider cases in which profitability of horizontal transmission, n, is higher. In these cases, we see a deviation from the pattern established in the previous subsection (lower n). Specifically, the stable expressions show a noticeable local peak for higher rates of vertical transmission, v, and lower birth rate, b_s (Figure 2.4). As an aside (for the moment), near the local peak, we lose the numerical data because our algorithm converges to an evolutionary equilibrium where there is effectively

no infection. The loss of numerical data is evidence by wire-frames in Figure 2.4 where v is large and b_s is relatively small. Biologically speaking, wire-frames are where selection driven extinction of pathogen occurs.

The local peak we identify can be characterized in two distinct ways. First, for a fixed birth rate, b_s, increasing v eventually triggers a rise in the level of trait expression (Figure 2.4). The intuition here is that, because we have a higher n, horizontal transmission is more profitable, so the pathogen-induced mortality is intencivized. It follows that the infected offspring produced by an infected host are at greater risk of pathogen-induced mortality. From the host parent's perspective, the risk is amplified as rates of vertical transmission increase, leading to increased recovery rate. Of course, increased recovery rate shortens the duration of infection, which encourages even more horizontal transmission and even greater pathogen-induced mortality.

Second, for a fixed vertical transmission rate, v, increasing birth rate, b_s, leads to a fall in the level of expression, at least near the peak (Figure 2.4). The intuition is that background mortality increases with birth rate, resulting in shorter host lifespan. Thus, increasing b_s may prompt a reduction in γ^* to preserve lifetime reproductive success over a shorter period of time. The changes we observe in the pathogen trait, α^*, could be viewed as a co-evolutionary response to the host. However, they do make sense on their own when we realize increasing b_s impacts expected duration of infection through its relationship with background mortality rate. As b_s intensifies, infections become shorter-lived, but opportunities for vertical transmission become more frequent as offspring are produced more quickly; this leads to the fall in α^* we see near the peak.

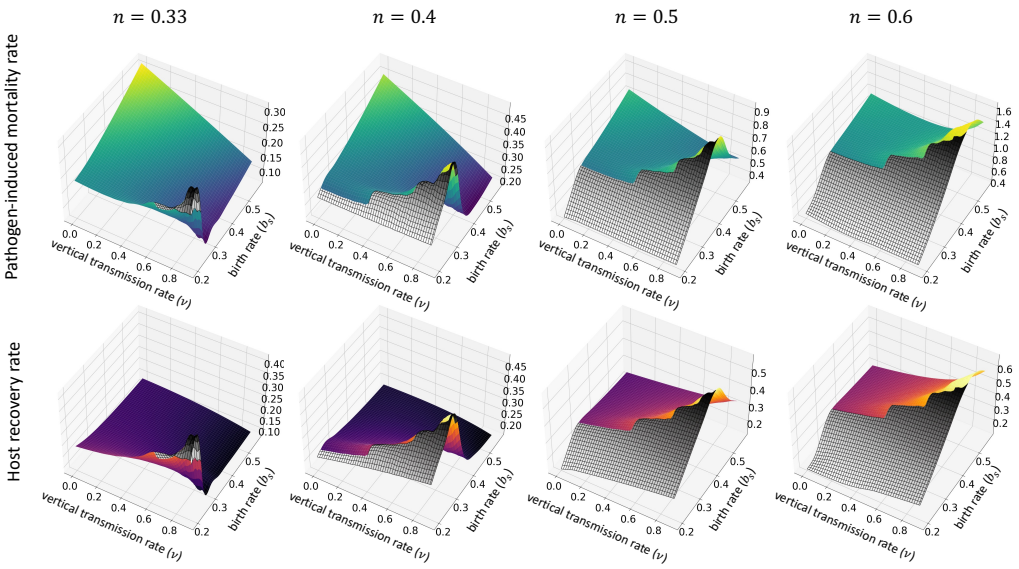

Figure 2.4: Variation in the evolutionarily stable values of the pathogen-induced mortality rate (α^*) and the host recovery rate (γ^*) in relation to different levels of vertical transmission rate (v) and birth rate (b_s) under distinct higher values of horizontal transmission profitability (n), specifically for $n = 0.33, 0.4, 0.5$, and 0.6. We observe a notable rise in these values at higher v levels. We assume the rate of exposed hosts becoming infectious, $\delta = 1$, and the background mortality rate, $\mu(N) = 0.15 \times N$, when N represents the total population. The grey wire-frames represent the regions where the number of infections is effectively zero, so we consider the pathogen to be extinct.

2.6.3 Virulence

We now explore the evolution of virulence defined in two distinct ways. The first definition of virulence we explore is related to case mortality, in other words the probability of an infectious host's death due to its infection (Day, 2002). The second definition is related to the fitness reduction experienced by a host when it acquires an infection (Read, 1994).

Case mortality, the probability of an infectious host dying from its infection, is calculated as

$$\frac{\alpha^*}{\alpha^* + \gamma^* + \mu(\bar{N})}, \tag{2.6.1}$$

where the superscript '$*$' reminds us that the expression is evaluated at the co-evolutionary equilibrium. Figure 2.5 shows how virulence, measured as case mortality, changes with the birth rate, b_s, vertical transmission rate, v, and also the horizontal transmission profitability, n. The relationship between case mortality and model parameters closely resembles that between pathogen-induced mortality, α^*, and model parameters (compare to Figures 2.4 and 2.3).

There are two additional noteworthy observations to be made about case mortality. First, it can increase as the rate of vertical transmission, v, goes up. Because, the highest case mortality occurs when (but not only when) there is no vertical transmission, any such rise in case mortality is preceded by a reduction (Figure 2.5). This first noteworthy observation is consistent with the findings of Shillcock et al. (2023) in a model with no self regulation of host population.

The second noteworthy observation is that when there is no vertical transmission, the case mortality at evolutionary equilibrium equals the profitability of horizontal transmission, captured by the parameter n. The same result was obtained by Day and Burns (2003) but with a model that, like Shillcock et al. (2023), lacked self regulation of the host population. In other words, the evolution of case mortality is completely determined by the shape of the trade-off between the rates of horizontal transmission and pathogen-induced mortality when $v = 0$. The result, here, is due to the functional form we chose for $\beta(\alpha)$. It is easy to prove, mathematically, that case mortality must equal n given our model for $\beta(\alpha)$ and given that the pathogen expresses 'α' at an evolutionary equilibrium level. The same is true for previous

work (Day and Burns, 2003; Shillcock et al., 2023).

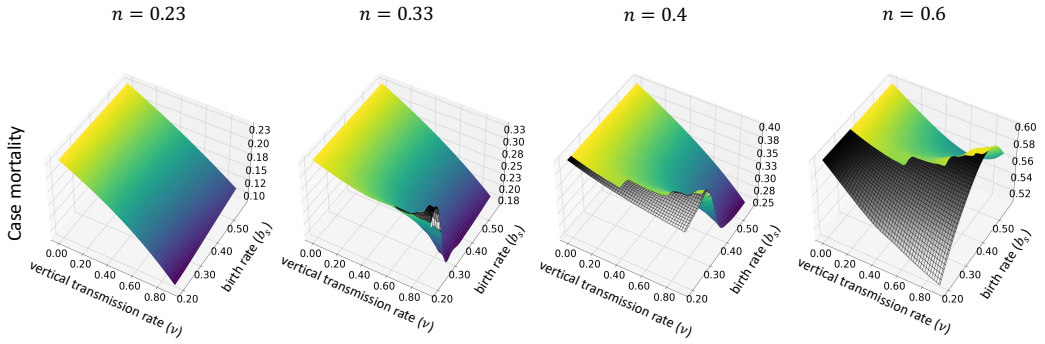

Figure 2.5: Variation in virulence as case mortality, which is calculated at co-evolutionary equilibrium, across a range of vertical transmission (v) and birth rates (b_s), evaluated at different values of horizontal transmission profitability (n), specifically for $n = 0.23, 0.33, 0.4$, and 0.6. Each subplot represents how virulence adapts with increasing n. We assume the rate of exposed hosts becoming infectious, $\delta = 1$, and the background mortality rate, $\mu(N) = 0.15 \times N$. The grey wire-frames represent the regions where the number of infections is effectively zero, so we consider the pathogen to be extinct.

The second definition of virulence we consider is the reduction in fitness experienced by a host who moves from the susceptible category to the exposed. In Appendix (A), we show that virulence in the second sense is expressed as

$$\frac{b_s - \mu(\bar{N})}{\beta(\alpha^*)\bar{I}}. \tag{2.6.2}$$

This mathematical definition of virulence differs from the analogous one found in Shillcock et al. (2023). However, the difference is not related to the presence or absence of self regulation of host population. It is related to the absence of an exposed class of host in Shillcock et al. (2023) model. Despite the differences between our mathematical definition of virulence (in the sense of fitness reduction) and that of

Shillcock et al. (2023), our qualitative predictions match theirs. In particular, virulence can increase with increasing vertical transmission, and this increase can lead virulence to exceed the levels at which it is observed that the vertical transmission is absent (Figure 2.6).

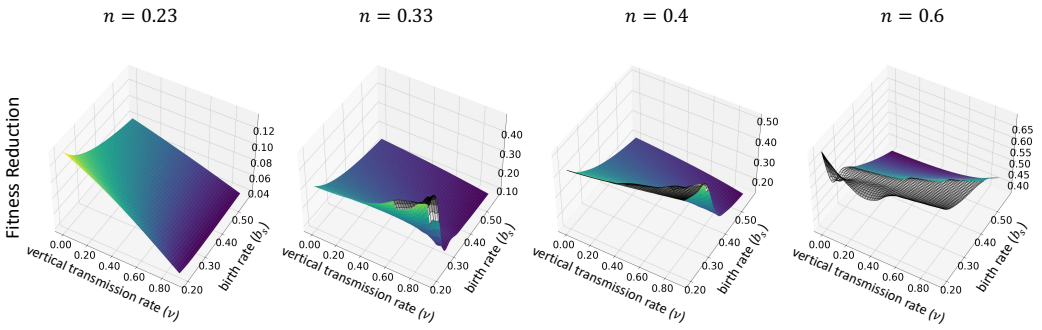

Figure 2.6: Variation in virulence as fitness reduction across a range of vertical transmission (v) and birth rates (b_s), evaluated at different values of horizontal transmission profitability (n), specifically for $n = 0.23, 0.33, 0.4$, and 0.6. Each subplot represents how virulence adapts with increasing n. We assume the rate of exposed hosts becoming infectious, $\delta = 1$, and the background mortality rate, $\mu(N) = 0.15 \times N$, when N represents the total population. The grey wire-frames represent the regions where the number of infections is effectively zero, so we consider the pathogen to be extinct.

2.7 Discussion

We have modelled the co-evolution of pathogen and its host when the former is both transmitted vertically and horizontally. Previous work neglects the possibility that host population growth may be limited by factors other than pathogen-induced mortality alone (Shillcock et al., 2023). In general, host population growth can be regulated in many ways. We want to understand how and whether co-evolutionary

predictions change when host population growth is constrained by factors beyond the pathogen alone.

One thing that does not change when we add self regulation of host population growth to a co-evolutionary model is the conclusion that increasing the vertical transmission rate does not always produce more benign disease outcomes. We find that increasing vertical transmission rate can lead to higher levels of pathogen-induced mortality. Like previous work that neglected non-linear features of host population growth (Shillcock et al., 2023), we find more benign disease outcomes evolve more readily when the horizontal transmission is more profitable to the pathogen. Unlike that previous work, though, we find that more benign outcomes are no longer closely connected to high rates of host reproduction. The contrast that our work provides stems from our model of negative density-dependent host population growth. We modelled this as density-dependent mortality and saw that increases in host birth rate were balanced by higher death rates. Ultimately, then, increases in host birth rate became associated with shorter infections which, we argue, intensifies the need for a pathogen to exploit its host and raises the risk of infection. The similarities and differences between the conclusions of our work and those of previous work (Shillcock et al., 2023), extend to the predicted levels of co-evolved virulence.

Vertical transmission does not always lead to more benign pathogens, but this does not mean that more benign pathogens are never the co-evolutionary result of vertical transmission. Previous theory has hinted that host-pathogen co-evolution might lead to very low levels of host harm when vertical transmission is possible (Shillcock et al., 2023). However, the hints are just that: hints. Previous theory is limited by the assumption that the pathogen is the only regulator of host population growth.

If pathogen-induced mortality and host recovery become too low, then previous theory has nothing to say, because there is no endemic equilibrium to serve as the central focus of an analysis. Therefore, if we want to uncover what happens when more benign pathogens co-evolve with their hosts, we need to add non-linear density dependent regulators of host population growth (van Baalen, 1998). In this paper, we do exactly this. We find that there are indeed co-evolutionary outcomes where host recovery and pathogen-induced mortality rate are low, and in those cases, the infection occurs at numbers that are positive but effectively zero. We interpret this result as selection-driven extinction of the pathogen, because low number of infectious hosts implies an elevated risk of stochastic loss of the pathogen (Dieckmann and Metz, 2006). Like van Baalen (1998), we find that density dependent regulation of the host population growth allows the host to drive the pathogen to extinction without going extinct itself. One might argue that this density dependence is key to achieving selection-driven extinction, because it implies invasion fitness of the host and pathogen, respectively, depends on resident traits. As previous authors argue, when invasion fitness is independent of resident traits— as it is in the model developed by Shillcock et al. (2023)— selection maximizes the population mean fitness making selection-driven extinction impossible (Matsuda and Abrams, 1994; but see Parvinen and Dieckmann, 2013, for clarity on selection-driven extinction under optimizing selection).

Unlike van Baalen (1998), our model allows for vertical transmission of the pathogen. Clearly then, vertical transmission is not necessary for selection-driven extinction of the pathogen to occur. However, our results show that selection-driven extinction of the pathogen does occur more readily when vertical transmission leads to high virulence, measured as a reduction in host fitness in a resident population. In other words, vertical transmission is more strongly associated with selection-driven

extinction of the pathogen when the fitness reduction experienced by infected hosts is high. This in turn is indicative of a greater competitive ecological advantage for susceptible hosts. Previous ecological models have predicted susceptible hosts can out-compete infected ones leading to the extinction of vertically transmitted parasites (Hochberg, 1991). Our work shows that similar predictions arise as a result of co-evolutionary forces.

A general prediction of our model is that pathogen-induced mortality and overall virulence increase when horizontal transmission becomes more profitable for the pathogen. This prediction holds even in the presence of the substantial vertical transmission. Our prediction is analogous to ones made about the impact of so-called 'imperfect vaccines' on pathogen evolution. An imperfect vaccine reduces the overall costs of virulence to pathogens, for example by lowering the mortality rate without limiting horizontal transmission (Gandon et al., 2001; Read et al., 2015; Fleming-Davies et al., 2018). In other words, an imperfect vaccine provides a pathogen with an incentive to exploit its host to a greater degree. In the context of our model, such an incentive arises as we increase the parameter n. Increasing this parameter raises the benefits of host exploitation holding the cost fixed.

Our general prediction, that virulence rises as horizontal transmission becomes more profitable, is also consistent with experimental findings. More to the point, it is consistent with experimental reductions in virulence that emerge when horizontal transmission becomes less profitable because it is prevented (Bull et al., 1991). It is also consistent with experimental results of Stewart et al. (2005) and Pagán et al. (2014) who found a positive relationship between horizontal transmission and pathogen virulence. Pagán et al. (2014) also demonstrated that plant viruses transmitted horizontally evolved to be more virulent than those transmitted vertically.

Our findings are limited by our modeling assumptions. One key limitation of our model is the assumption that hosts can only be infected by a single strain of pathogen at any given time. Our model, therefore, does not account for the possibility of co-infections with multiple pathogen strains. If co-infecting strains did occur and were distantly related, we would expect even higher levels of pathogen trait expression to evolve because each strain would be more inclined to pursue selfish interests (Frank, 1992). In this case, we also speculate the level of host trait expression (recovery) would increase in response to more aggressive disease-causing agent.

Another key limitation of our model is the assumption that mutations in the host population are independent of those in the pathogen population. This means we neglect the potential for phenotypic correlations between hosts and pathogens to emerge. Positive phenotypic correlations between social partners –e.g. a pathogen and its host– is known to produce cooperative evolutionary outcomes (Fletcher and Doebeli, 2009a). Thus, if we were to allow these correlations in our model, they would likely drive trait expressions to lower levels. Similar predictions are made by models built around sequential move evolutionary games that allow positive phenotypic correlations between host and pathogen to emerge (Taylor et al., 2006). Whether low levels of trait expressions in these cases lead to pathogen extinction is an open question.

Finally, we assumed host population growth is regulated by background mortality that is density-dependent. As we have explained, this modelling decision means that the duration of infection is sensitive to host demography. In other words, a particular life history feature of the pathogen is sensitive to changes in the host population size. Had we incorporated density dependent host birth rates instead,

duration of infection would have been independent of host population size. In this case, the incentives that shape the evolution of pathogen trait expression may be quite different. Future work should focus on outlining the role of density dependent demography of co-evolution of hosts and their vertically transmitted pathogens.

Chapter 3

Conclusion

3.1 Summary

Understanding the impact of vertical transmission on pathogen-host co-evolution is crucial for public health and ecosystem balance. Previous work indicates that vertical transmission can sometimes bring co-evolving pathogens and hosts into greater conflict, contrary to widely accepted views. However, this work is based on a model where pathogen-induced mortality alone regulates the host population, which can result in unbounded host population growth if the pathogen-induced mortality is too low or absent, failing to address phenomena like selection-driven extinction of pathogens.

In the second chapter, I modeled the co-evolution of pathogens and their hosts with both vertical and horizontal transmission, incorporating density-dependent host population growth. To achieve this, I explored the dynamics of host-pathogen interactions using evolutionary game theory and adaptive dynamics. I found that

increasing vertical transmission does not always result in more benign disease outcomes; instead, it can lead to higher pathogen-induced mortality. Furthermore, more benign outcomes evolve more readily when horizontal transmission is more profitable for the pathogen, and overall virulence increases as horizontal transmission becomes more profitable. Unlike previous models that assumed pathogen-induced mortality as the sole regulator, my approach showed that increased host birth rates, balanced by higher death rates, can shorten infections and intensify pathogen exploitation. The results also indicated that vertical transmission, when associated with high virulence, can drive selection-driven extinction of the pathogen, which highlights the importance of considering both transmission modes in disease management strategies.

3.2 Where to Go From Here?

In this study, I made several assumptions that, while simplifying the model, might limit its applicability. It would be beneficial for future research to focus on relaxing some of these assumptions to obtain a more comprehensive understanding of host-pathogen dynamics. I also mention a few potential extension to my model for future work.

First of all, I have neglected the possibility of co-infection, meaning that I assume each host can only be infected by a single strain of a pathogen at any given time. However, previous research has shown that co-infection can significantly impact the evolution of virulence. For example, Frank (1992) developed a model that explores how the relatedness of co-infecting strains affects virulence. His model suggests that when genetically distinct strains infect the same host, competition among these strains can drive the evolution of higher virulence. Additionally, I have imposed

the limitation that once a host is infected by a pathogen strain, it cannot be subsequently infected by a more virulent strain. This restriction contrasts with models that allow superinfection. According to Nowak and May (1994), allowing superinfection leads to intra-host competition among different strains of the pathogen, driving the evolution of increased virulence as more aggressive strains outcompete less virulent ones. This results in higher levels of virulence overall but can also lead to a reduction in transmission rates due to increased host damage. This simplification allows us to focus on the dynamics of single-strain infections without the added complexity of interactions between multiple strains within the same host. However, this simplification is a limitation of my current work. Future research could extend this model to include the possibility of superinfection to allow for a more comprehensive exploration of how intra-host competition among multiple pathogen strains influences virulence evolution.

Another key limitation of my model is the assumption that mutations in the host population are independent of those in the pathogen population. This neglects the potential for phenotypic correlations between hosts and pathogens. Positive phenotypic correlations between social partners, such as a pathogen and its host, are known to produce cooperative evolutionary outcomes. For example, Fletcher and Doebeli (2009b) demonstrate how positive phenotypic correlations can drive the evolution of cooperative behaviors. Taylor et al. (2006) explores a case of host-pathogen interaction where cooperation leads to reduced levels of virulence in pathogens. Conversely, negative phenotypic correlations between host and pathogen traits can drive the evolution of increased virulence as pathogens adapt to exploit hosts more effectively. As another example of cooperative behavior, Sanchez et al. (2018) found that metabolic adaptations in the host, as a cooperative defense, could create an environment that supports the pathogen's presence without causing sig-

nificant harm, leading to a state where the pathogen can persist without triggering severe disease symptoms. Future work could explore how virulence might evolve under scenarios of both positive and negative phenotypic correlations, particularly examining how cooperation between hosts and pathogens, allowing vertical transmission combined with different levels of horizontal transmission profitability, influences evolutionary outcomes.

For this model, I suggest a modification to the birth rate of infectious individuals, $b_I(\gamma)$, to incorporate a cost associated with host recovery. Instead of $b_I(\gamma) = b_s - \gamma^2$, I propose using $b_I(\gamma) = b_s - \lambda\gamma^2$, where λ represents the cost coefficient of recovery. This change allows exploration of how recovery costs impact pathogen and host dynamics. As λ increases, $\lambda\gamma^2$ significantly reduces the birth rate of infected hosts at higher recovery rates, making high recovery rates less favorable for pathogens. Shillcock et al. (2023) explored various costs for the host to clear infection, showing more benign outcomes when recovery was costlier to the host. This could be due to the evolution of lower recovery rates, resulting in longer infectious periods and pathogens evolving lower virulence to balance prolonged infection benefits against harmful effects on host reproduction. Hosts can evolve resistance or tolerance; high immune response costs sometimes lead to tolerance rather than resistance. It would be interesting to see how modifying costs in our model impacts trait expressions and virulence. These insights into recovery cost trade-offs could inform new strategies for managing infections.

Another suggestion for future work is to explore my findings on selection-driven extinction outcomes in greater detail. I discovered that more profitable horizontal transmission could allow for selection-driven extinction of the pathogen across a broader range of parameters, such as vertical transmission and birth rates. On the

other hand, as discussed, an imperfect vaccine reduces the overall costs of virulence to pathogens by lowering mortality rates without limiting horizontal transmission (Gandon et al., 2001; Fleming-Davies et al., 2018; Read et al., 2015). This reduction provides pathogens with an incentive to exploit their hosts more, represented in my model by increasing the horizontal transmission profitability, parameter n, which raises the benefits of host exploitation while keeping the cost fixed. This raises the question: Could an imperfect vaccine potentially increase the likelihood of pathogen extinction, similar to my finding of more potential pathogen extinction for higher n? Future research could investigate whether the increased exploitation incentives introduced by imperfect vaccines might lead to a higher chance of pathogen extinction, providing important insights for vaccine strategy and disease management. Additionally, it would be worthwhile to explore any potential correlation between higher levels of virulence and increased potential for pathogen extinction. Higher virulence has been found for high horizontal profitability (Stewart et al., 2005; Pagán et al., 2014). If a correlation exists, it might be feasible to utilize this as a means of disease management to drive the pathogen to extinction.

In conclusion, my study emphasizes the importance of considering various factors such as recovery costs, coinfection dynamics, and phenotypic correlations in modeling host-pathogen interactions. Future work should empirically validate these theoretical insights. Refining my model to include these factors will enhance our understanding of disease dynamics and inform better strategies for managing infectious diseases. This comprehensive approach will provide a more accurate and robust framework for predicting and controlling pathogen behavior in different ecological and evolutionary contexts.

Bibliography

Abrams, P.A., Matsuda, H., Harada, Y., 1993. Evolutionary unstable fitness maxima and stable fitness minima of continuous traits. Evolutionary Ecology 7, 465–487. doi:10.1007/BF01237642.

Acevedo, M.A., Dillemuth, F.P., Flick, A.J., Faldyn, M.J., Elderd, B.D., 2019. Virulence-driven trade-offs in disease transmission: A meta-analysis. Evolution 73, 636–647. doi:10.1111/evo.13692.

Alizon, S., Hurford, A., Mideo, N., Van Baalen, M., 2009. Virulence evolution and the trade-off hypothesis: history, current state of affairs and the future. Journal of Evolutionary Biology 22, 245–259. doi:10.1111/j.1420-9101.2008.01658.x.

Arora, N., McDonald, S., Reichert, M., Cohen, C., 2022. Microbial vertical transmission during human pregnancy. Journal of Perinatology 42, 1102–1110. doi:10.1038/s41372-022-01331-9.

Britton, N.F., 2003. Essential Mathematical Biology. Springer. doi:10.1007/978-1-4471-0049-2.

Bull, J.J., Molineux, I.J., Rice, W.R., 1991. Selection of benevolence in a host–parasite system. Evolution 45, 875–882.

Christiansen, F.B., 1991. On conditions for evolutionary stability for a continuously varying character. The American Naturalist 138, 37–50. URL: https://www.jstor.org/stable/2462531, doi:10.1086/285206.

Cressler, C.E., McLeod, D.V., Rozins, C., Van Den Hoogen, J., Day, T., 2016. The adaptive evolution of virulence: a review of theoretical predictions and empirical tests. Parasitology 143, 915–930. doi:10.1017/S003118201500092X.

Day, T., 2002. On the evolution of virulence and the relationship between various measures of mortality. Proceedings of the Royal Society, B 269, 1317–1323. doi:10.1098/rspb.2002.2021.

Day, T., Burns, J., 2003. A consideration of patterns of virulence arising from host-parasite coevolution. Evolution 57, 671–676. doi:10.1111/j.0014-3820.2003.tb01558.x.

Dercole, F., Rinaldi, S., 2008. Analysis of Evolutionary Processes: The Adaptive Dynamics Approach and Its Applications. Princeton University Press, Princeton, NJ.

Dieckmann, U., Law, R., 1996. The dynamical theory of coevolution: a derivation from stochastic ecological processes. Journal of Mathematical Biology 34, 579–612. doi:10.1007/BF02409751.

Dieckmann, U., Metz, J.A.J., 2006. Surprising evolutionary predictions from enhanced ecological realism. Theoretical Population Biology 69, 263–281. doi:10.1016/j.tpb.2005.12.001.

van den Driessche, P., Watmough, J., 2002. Reproduction numbers and sub-threshold endemic equilibria for compartmental models of disease transmission. Mathematical Biosciences 180, 29–48. doi:10.1016/s0025-5564(02)00108-6.

Eshel, I., 1983. Evolutionary and continuous stability. Journal of Theoretical Biology 103, 99–111. doi:10.1016/0022-5193(83)90201-1.

Eshel, I., Motro, U., 1981. Kin selection and strong evolutionary stability of mutual help. Theoretical Population Biology 19, 420–433. doi:10.1016/0040-5809(81)90031-9.

Ewald, P.W., 1994. Evolution of Infectious Disease. Oxford University Press, Oxford.

Fleming-Davies, A.E., Williams, P.D., Dhondt, A.A., Dobson, A.P., Hochachka, W.M., Leon, A.E., Ley, D.H., Osnas, E.E., Hawley, D.M., 2018. Incomplete host immunity favors the evolution of virulence in an emergent pathogen. Science 359, 1030–1033. doi:10.1126/science.aao2140.

Fletcher, J.A., Doebeli, M., 2009a. A simple and general explanation for the evolution of altruism. Proceedings of the Royal Society, B 276, 13–19. doi:10.1098/rspb.2008.0829.

Fletcher, J.A., Doebeli, M., 2009b. A simple and general explanation for the evolution of altruism. Proceedings of the Royal Society, B 276, 13–19.

Frank, S.A., 1992. A kin selection model for the evolution of virulence. Proceedings of the Royal Society, B 250, 195–197.

Frank, S.A., 1996. Models of parasite virulence. The Quarterly Review of Biology 71, 37–78.

Gandon, S., Mackinnon, M.J., Nee, S., Read, A.F., 2001. Imperfect vaccines and the evolution of pathogen virulence. Nature 414, 751–756.

Geritz, S., Kisdi, E., Meszena, G., Metz, J., 1998. Evolutionarily singular strategies and the adaptive growth and branching of the evolutionary tree. Evolutionary Ecology 12, 35–57. doi:10.1023/A:1006554906681.

Godfray, H., 1994. Parasitoids: Behavioral and Evolutionary Ecology. Princeton University Press.

Hochberg, M., 1991. Population dynamic consequences of the interplay between parasitism and intraspecific competition for host-parasite systems. Oikos 61, 297–306. doi:10.2307/3545237.

Hurford, A., Cownden, D., Day, T., 2009. Next-generation tools for evolutionary invasion analyses. Journal of The Royal Society Interface 7, 561–571. doi:10.1098/rsif.2009.0448.

Lipsitch, M., Nowak, M.A., Ebert, D., May, R.M., 1996. The population dynamics of vertically and horizontally transmitted parasites. Proceedings of the Royal Society B: Biological Sciences 263, 2105–2116. doi:10.1098/rspb.1996.0245.

Matsuda, H., Abrams, P., 1994. Timid consumers: self-extinction due to adaptive change in forging and anti-predator effort. Theoretical Population Biology 45, 76–91. doi:10.1006/tpbi.1994.1004.

Maynard Smith, J., 1982. Evolution and the Theory of Games. Cambridge University Press.

Maynard Smith, J., Price, G.R., 1973. The logic of animal conflict. Nature 246, 1476–4687. doi:10.1111/j.1096-3642.1935.tb01680.x.

Metz, J., Nisbet, R., Geritz, S., 1992. How should we define 'fitness' for general ecological scenarios? Trends in Ecology and Evolution 7, 198–202. doi:10.1016/0169-5347(92)90073-K.

Montoya, J., Liesenfeld, O., 2004. Toxoplasmosis. Lancet 363, 1965–1976. doi:10.1016/S0140-6736(04)16412-X.

Nicholson, A., Bailey, V., 1935. The balance of animal populations. Proceedings of the Zoological Society of London 105, 551–598. doi:10.1038/246015a0.

Nowak, M.A., May, R.M., 1994. Superinfection and the evolution of parasite virulence. Proceedings of the Royal Society, B 255, 81–89.

Pagán, I., Montes, N., Milgroom, M.G., García-Arenal, F., 2014. Vertical transmission selects for reduced virulence in a plant virus and for increased resistance in the host. PLoS Pathogens 10, e1004293. doi:10.1371/journal.ppat.1004293.

Pagán, I., Montes, N., Milgroom, M.G., García-Arenal, F., 2022. Transmission of plant viruses through seeds. Annual Review of Phytopathology 60, 77–96. doi:10.1146/annurev-phyto-021621-105024.

Parvinen, K., Dieckmann, U., 2013. Self-extinction through optimizing selection. Journal of Theoretical Biology 333, 1–9. doi:10.1016/j.jtbi.2013.03.025.

Price, P.W., 1980. Evolutionary Biology of Parasites. Princeton University Press, Princeton, NJ.

Read, A.F., 1994. The evolution of virulence. Trends in Microbiology 2, 73–76. doi:10.1016/0966-842X(94)90537-1.

Read, A.F., Baigent, S.J., Powers, C., Kgosana, L.B., Blackwell, L., Smith, L.P., Kennedy, D.A., Walkden-Brown, S.W., Nair, V.K., 2015. Imperfect vaccination

can enhance the transmission of highly virulent pathogens. PLoS Biology 13, e1002198. doi:10.1371/journal.pbio.1002198.

Sanchez, K.K., Chen, G.Y., Schieber, A.M.P., Redford, S.E., Shokhirev, M.N., et al., 2018. Cooperative metabolic adaptations in the host can favor asymptomatic infection and select for attenuated virulence in an enteric pathogen. Cell 175, 146–158.

Shillcock, G., Úbeda, F., Wild, G., 2023. Vertical transmission does not always lead to benign pathogen–host associations. Evolution Letters 7, 305–314. doi:10.1093/evlett/qrad028.

Stearns, S.C., Medzhitov, R., 2015. Evolutionary Medicine. Sinauer Associates, Sunderland, MA. doi:10.1093/med/9780199661695.001.0001.

Stewart, A.D., Logsdon, J.M., Kelley, S.E., 2005. An empirical study of the evolution of virulence under both horizontal and vertical transmission. Evolution 59, 730–739. doi:10.1554/03-330.

Taylor, P., Day, T., Nagy, D., Wild, G., André, J.B., Gardner, A., 2006. The evolutionary consequences of plasticity in host-pathogen interactions. Theoretical Population Biology 69, 323–331. doi:10.1016/j.tpb.2005.09.004.

Taylor, P.D., 1996. Inclusive fitness arguments in genetic models of behaviour. Journal of Mathematical Biology 34, 654–674. doi:10.1007/BF02409753.

van Baalen, M., 1998. Coevolution of recovery ability and virulence. Proceedings of the Royal Society, B 265, 317 – 325.

Werren, J.H., 1997. Wolbachia and the biology of reproductive parasites. Nature Reviews Genetics 1, 55–64. doi:10.1038/nrg1202.

Úbeda, F., Jansen, V.A.A., 2016. The evolution of sex-specific virulence in infectious diseases. Nature Communications 7, 13849. doi:10.1038/ncomms13849.

Appendices

A Virulence (Fitness Reduction)

Here, we derive the function for virulence as a measure of fitness reduction. To do this, we need to find how much the susceptible host's fitness is reduced when it gets exposed to an infection. We know that at equilibrium the fitness change of all populations (susceptible, exposed, infectious) should be zero, which means that:

$$\begin{bmatrix} \frac{dW_S}{dt} \\ \frac{dW_E}{dt} \\ \frac{dW_I}{dt} \end{bmatrix} = J_h \begin{bmatrix} W_S \\ W_E \\ W_I \end{bmatrix} = \begin{bmatrix} 0 \\ 0 \\ 0 \end{bmatrix}, \tag{A.1}$$

where W_S, W_E, and W_I denote the host fitness when it is susceptible, exposed, and infectious, respectively. We also previously computed J_h (2.3.10). So we have:

$$\begin{bmatrix} W_S \\ W_E \\ W_I \end{bmatrix} \begin{bmatrix} b_s - \beta(\alpha)\bar{I} - \mu(\bar{N}) & b_s & (1-v)b_I(\gamma_m) + \gamma_m \\ \beta(\alpha)\bar{I} & -\delta - \mu(\bar{N}) & vb_I(\gamma_m) \\ 0 & \delta & -(\gamma_m + \alpha + \mu(\bar{N})) \end{bmatrix} = \begin{bmatrix} 0 \\ 0 \\ 0 \end{bmatrix}.$$

Knowing that $W_S = 1$, we solve for W_E:

$$W_E = \frac{\beta(\alpha)\bar{I} - (b_s - \mu(\bar{N}))}{\beta(\alpha)\bar{I}}.$$

Thus, the fitness reduction would be:

$$1 - W_E = \frac{b_s - \mu(\bar{N})}{\beta(\alpha)\bar{I}}.$$

B Jupyter Notebook Implementation

This appendix contains the Jupyter Notebook, which includes the complete implementation details of the methods and analyses discussed in the second chapter. Each step of the implementation is thoroughly documented with code snippets and explanations to enhance understanding and reproducibility.

0.0.1 Libraries

In the following cell, we import essential libraries for numerical operations, data handling, and visualization.

[2]:
```
import numpy as np
from scipy.integrate import odeint
import matplotlib.pyplot as plt
import pandas as pd
import csv
from scipy.interpolate import griddata
from mpl_toolkits.mplot3d import Axes3D
```

0.0.2 Notation Key

`alpha`: pathogen_induced mortality rate (resident)
`gamma`: host recovery rate (resident)
`alpha_m`: pathogen-induced mortality rate (mutant)
`gamma_m`: host recovery rate (mutant)
`bs`: birth rate of non-infectious individuals
`mu`: background mortality rate
`mu_coef`(μ_0): coefficient of background mortality rate
`beta`: horizontal transmission rate constant
`delta`: the rate at which the exposed population gets infectious
`N`: total population
`bI`: birth rate of infectious individuals
`n`: profitability of the horizontal transmission to the pathogen
`S`, `E`, `I`: susceptible, exposed, and infectious population size
`z : (S, E, I)`
`v`: vertical transmission rate
`Wp`: pathogen fitness function
`Wh`: host fitness function
`eps`: epsilon
`niter`: number of iteration

0.0.3 Defining Key Functions

In the following code snippet, we define several crucial functions required for simulating and analyzing the dynamics of our model.

- **`bI(gamma, bs)`**: Calculates the birth rate of the infectious population based on the host recovery rate (γ) denoted by `gamma` and the basic birth rate (b_s) denoted by `bs`.
- **`mu(N, mu_coef = 0.15)`**: Computes the background mortality rate as a function of the total population (`N`) scaled by a coefficient, μ_0, represented by `mu_coef`.
- **`beta(alpha, n)`**: Determines the horizontal transmission rate constant, as a function of the pathogen-induced mortality rate ('α'), denoted by `alpha`, and `n` (which represents the profitability of the horizontal transmission to the pathogen).
- **`population_rates(z, gamma, alpha, bs, v, n, delta=1, mu_coef = 0.15)`**: Represents the population model, calculating the rate of change of susceptible (`S`), exposed (`E`), and infectious (`I`) population sized over time given a set of parameters.
- **`endemic_equilibrium(z, gamma, alpha, bs, v, n)`**: Returns the endemic equilibrium of the population, by an iterative process of updating $\frac{dz}{dt}$ and adjusting `z` based on that so that the magnitude of the gradient falls below a specified threshold, indicating convergence to an optimal point. The rates of change are calculated at each iteration using the `population_rates` function.
- **`Wh(z, gamma_m, alpha, bs, v, n, delta=1)`** and **`Wp(z, gamma, alpha_m, bs, v, n, delta=1)`**: Calculate the fitness of the host and the pathogen, respectively, given sets of parameters.
- **`gradient_fitness_pathogen(z, gamma, alpha, bs, v, n, eps)`** and **`gradient_fitness_host(z, gamma, alpha, bs, v, n, eps)`**: Return the approximate gradients of the fitness functions, evaluated at the input parameters `gamma` and `alpha`, using the other provided parameter values.
- **`convergence_stable(z, gamma, alpha, bs, v, n)`**: Starting with an initial guess for stable α and γ, the endemic equilibrium is found using the `endemic_equilibrium` function. Then, it evaluates the fitness of the pathogen and the host at equilibrium using the `Wp` and `Wh` functions, respectively. Then, it calculates the fitness gradients. This iterative process continues, with updates to the evolutionary trait expressions, until the gradients approach a tolerance level near zero. The procedure returns the convergence stable γ and α, along with other information, based on a given set of parameters.
- **`ESS(gradient_fitness_pathogen, gradient_fitness_host)`**: Evaluate whether both fitness gradients are less than zero to confirm the presence of an Evolutionarily Stable Strategy (ESS). It returns 1 if an ESS is confirmed and 0 otherwise.

[8]:
```
# Function to calculate the adjusted birth rate of infectious individuals
def bI(gamma, bs):
    return bs - (gamma**2)

# Function to calculate the background mortality rate based on total population
def mu(N, mu_coef=0.15):
    return mu_coef * N

# Function to calculate the rate constant of horizontal transmission
def beta(alpha, n):
```

```
    return alpha ** n

# Main function to calculate the rates of change in population classes
def population_rates(z, gamma, alpha, bs, v, n, delta=1, mu_coef=0.15):
    N = np.sum(z)  # Summing up the population to get total N
    mu_val = mu(N)
    beta_val = beta(alpha, n)
    bI_val = bI(gamma, bs)

    # Differential equations representing the changes in susceptible, exposed,␣
 ↪and infectious populations
    dSdt = bs * z[0] + bs * z[1] + (1 - v) * bI_val * z[2] - beta_val * z[2] *␣
 ↪z[0] + gamma * z[2] - mu_val * z[0]
    dEdt = beta_val * z[2] * z[0] + v * bI_val * z[2] - delta * z[1] - mu_val *␣
 ↪z[1]
    dIdt = delta * z[1] - gamma * z[2] - alpha * z[2] - mu_val * z[2]

    dzdt = np.array([dSdt, dEdt, dIdt])
    return dzdt

# Function to find the equilibrium state of the population
def endemic_equilibrium(z, gamma, alpha, bs, v, n):
    N = np.sum(z)
    dzdt = np.array([1.0, 0.01, 0.0]) #initializing dz/dt

    # Iteratively finding the equilibrium state until changes are below the␣
 ↪threshold
    while np.max(np.abs(dzdt)) > 1e-05:
        dzdt = population_rates(z, gamma, alpha, bs, v, n)
        z += 0.01 * dzdt

    return z

# Function to calculate host fitness with mutant recovery rate
def Wh(z, gamma_m, alpha, bs, v, n, delta=1):
    N = np.sum(z)
    beta_val = beta(alpha, n)
    bI_val = bI(gamma_m, bs)
    mu_val = mu(N)

    F = np.array([[bs, bs, (1-v) * bI_val],
                  [0, 0, v * bI_val],
                  [0, 0, 0]])
    V = np.array([[z[2] * beta_val + mu_val, 0, -gamma_m],
                  [-z[2] * beta_val, delta + mu_val, 0],
                  [0, -delta, alpha + gamma_m + mu_val]])
```

```
    K = np.matmul(F, np.linalg.inv(V))
    return ((K[0][0] + K[1][1]) + np.sqrt((K[0][0] + K[1][1])**2 - 4 * (K[0][0]␣
 ↪* K[1][1] - K[1][0] * K[0][1]))) / 2

# Function to calculate pathogen fitness with mutant mortality rate
def Wp(z, gamma, alpha_m, bs, v, n, delta=1):
    N = np.sum(z)
    beta_val = beta(alpha_m, n)
    bI_val = bI(gamma, bs)
    mu_val = mu(N)

    return ((delta) / (delta + mu_val)) * (((beta_val * (z[0]) + v * bI_val)) /␣
 ↪(gamma + alpha_m + mu_val))

# Function to test convergence and stability of the system
def convergence_stable(z, gamma, alpha, bs, v, n):
    niter = 0
    tol = 1e-06
    eps = 0.0001

    while True:
        N = np.sum(z)
        niter += 1
        mu_val = mu(N)
        z = endemic_equilibrium(z, gamma, alpha, bs, v, n)

        Wh_up = Wh(z, gamma + eps, alpha, bs, v, n)  #Wh at gamma_m = gamma +␣
 ↪eps
        Wh_down = Wh(z, gamma - eps, alpha, bs, v, n) #Wh at gamma_m = gamma -␣
 ↪eps
        Gh = (Wh_up - Wh_down) / (2 * eps)

        Wp_up = Wp(z, gamma, alpha + eps, bs, v, n) #Wp at alpha_m = alpha + eps
        Wp_down = Wp(z, gamma, alpha - eps, bs, v, n) #Wp at alpha_m = alpha -␣
 ↪eps
        Gp = (Wp_up - Wp_down) / (2 * eps)

        #updating alpha & gamma using Gp & Gh
        gamma += 0.01 * Gh
        alpha += 0.01 * Gp

        if abs(Gh) < tol and abs(Gp) < tol:
            break

    return gamma, alpha, Gp, Gh, z
```

```
# Function to calculate the gradient of fitness for the host using the finite␣
 ↪different approximation
def gradient_fitness_host(z, gamma, alpha, bs, v, n, eps):
    return (Wh(z, gamma + 2 * eps, alpha, bs, v, n) - 2 * Wh(z, gamma, alpha,␣
 ↪bs, v, n) +
            Wh(z, gamma - 2 * eps, alpha, bs, v, n)) / (4 * (eps) ** 2)

# Function to calculate the gradient of fitness for pathogen using the finite␣
 ↪different approximation
def gradient_fitness_pathogen(z, gamma, alpha, bs, v, n, eps):
    return (Wp(z, gamma, alpha + 2 * eps, bs, v, n) - 2 * Wp(z, gamma, alpha,␣
 ↪bs, v, n) +
            Wp(z, gamma, alpha - 2 * eps, bs, v, n)) / (4 * (eps) ** 2)

# Function to determine if an evolutionarily stable strategy (ESS) is achieved
def ESS(gradient_fitness_pathogen, gradient_fitness_host):
    if gradient_fitness_pathogen < 0 and gradient_fitness_host < 0:
        return 1
    else:
        return 0
```

0.0.4 Creating CSV Data file

In the following code snippet, we first create a CSV file named `model_data.csv` with defined headers. We then loop over values of `bs`, `v`, and `n` values, adding records to the CSV file. (As the code execution is time-consuming and may be interrupted, I executed the code separately for each `n` value.)

[ ]:
```
# defining headers
headers = ["bs", "delta", "v", "gamma*", "alpha*", "S_bar", "E_bar","I_bar",␣
 ↪"N", "n", "beta", "bI", "Gp", "Gh", "mu", "ESS"]
# Create the CSV file and write headers
with open('model_data.csv', 'w', newline='') as file:
    writer = csv.writer(file)
    writer.writerow(headers)


# Loop over the specified n values
for n in [0.23, 0.27, 0.33, 0.36, 0.4, 0.5, 0.6, 0.7]:
    for bs in np.arange(0.2, 0.6, 0.04):
        for v in np.arange(0.0, 0.1, 0.05):

            gamma = 0.1
            alpha = 0.1
            eps_val = 0.001
            z = np.array([0.6, 0.2, 0.7])
```

```
            # Compute convergence stable and gradient fitness
            gamma, alpha, Gp, Gh, z = convergence_stable(z, gamma, alpha, bs,␣
↪v, n)
            gradient_fitness_pathogen_val = gradient_fitness_pathogen(z, gamma,␣
↪alpha, bs, v, n, eps_val)
            gradient_fitness_host_val = gradient_fitness_host(z, gamma, alpha,␣
↪bs, v, n, eps_val)

            # Determine if an Evolutionarily Stable Strategy (ESS) is achieved
            ESS_val = ESS(gradient_fitness_pathogen_val,␣
↪gradient_fitness_host_val)

            # Compute the total population at ESS
            N = z[0] + z[1] + z[2]

            # open the dataset and add a row
            with open('model_data.csv', 'a', newline='') as file:
              writer = csv.writer(file)
              writer.writerow([round(bs, 3), 1, round(v, 3), gamma, alpha,␣
↪z[0], z[1], z[2], N, round(n, 3), beta(alpha, n), bI(gamma, bs), Gp, Gh ,␣
↪mu(N), ESS_val])
```

0.0.5 Importing Data/ Adding Virulence

In the following code snippet, we import the dataset and augment it by adding new columns for case mortality and virulence (fitness reduction).

[5]:
```
import pandas as pd

# Load the dataset from a CSV file
df = pd.read_csv('model_data.csv')

# Compute fitness reduction as a new column named 'virulence'
df['virulence'] = (df["bs"] - df["mu"])/(df["beta"] * df["I_bar"])

# Compute case mortality rate and add it as a new column named 'case_mortality'
df['case_mortality'] = df['alpha*'] / (df['alpha*'] + df['gamma*'] + df['mu'])
```

0.0.6 Visualization

Here, we visualize the effects of variation in `n` (horizontal transmission profitability) on the pathogen-induced mortality rate and host recovery rate across different values of `v` (vertical transmission rate) and `bs` (birth rate).

[13]:
```
# Pre-defined values of 'n' for which analysis is conducted
n_values = [0.33, 0.4, 0.5, 0.6, 0.7]
```

```
# Filtering the dataframe for each 'n' value to create separate dataframes
df_beta023 = df[df['n'] == 0.23]
df_beta027 = df[df['n'] == 0.27]
df_beta030 = df[df['n'] == 0.3]
df_beta033 = df[df['n'] == 0.33]
df_beta036 = df[df['n'] == 0.36]
df_beta040 = df[df['n'] == 0.4]
df_beta050 = df[df['n'] == 0.5]
df_beta060 = df[df['n'] == 0.6]
df_beta070 = df[df['n'] == 0.7]

# Selecting dataframes for the analysis
dfs = [df_beta033, df_beta040, df_beta050, df_beta060, df_beta070]

# Setting up the figure for 3D plotting
fig = plt.figure(figsize=(70, 20))

# Loop through each selected dataframe and corresponding 'n' value
for i, (n, df_filtered) in enumerate(zip(n_values, dfs), start=1):
    # Create grid points for interpolation based on 'v' and 'bs' ranges
    xi = np.linspace(df_filtered['v'].min(), df_filtered['v'].max(), 100)
    yi = np.linspace(df_filtered['bs'].min(), df_filtered['bs'].max(), 100)
    xi, yi = np.meshgrid(xi, yi)

    # Interpolate alpha* and gamma* values for the grid
    zia = griddata((df_filtered['v'].dropna(), df_filtered['bs'].dropna()),␣
 ↪df_filtered['alpha*'].dropna(), (xi, yi), method='cubic')
    zig = griddata((df_filtered['v'].dropna(), df_filtered['bs'].dropna()),␣
 ↪df_filtered['gamma*'].dropna(), (xi, yi), method='cubic')

    # Apply masks based on various conditions to handle invalid or extreme data␣
 ↪points
    mask1 = griddata((df_filtered['v'], df_filtered['bs']), df_filtered['bI'] <␣
 ↪0, (xi, yi), method='nearest')
    mask2 = griddata((df_filtered['v'], df_filtered['bs']),␣
 ↪df_filtered['I_bar'] < 1e-3, (xi, yi), method='nearest')
    mask3 = griddata((df_filtered['v'], df_filtered['bs']),␣
 ↪df_filtered['E_bar'] < 1e-3, (xi, yi), method='nearest')
    mask_combined = mask2 | mask3

    # Set invalid data points to NaN for alpha* and gamma*
    zia[mask1] = np.nan
    zig[mask1] = np.nan

    # Plot alpha* values on a 3D surface plot
    ax1 = fig.add_subplot(2, len(n_values), i, projection='3d')
```

```
    surf_alpha_1 = ax1.plot_surface(xi, yi, zia, cmap='viridis',␣
↪edgecolor='none')
    ax1.plot_surface(xi, yi, np.where(mask_combined, zia, np.nan),␣
↪cmap='Greys', edgecolor='none', zorder=1)
    ax1.plot_wireframe(xi, yi, np.where(mask_combined, zia, np.nan),␣
↪color='black', alpha=0.7)
    ax1.set_xlabel(r'$(v)$', fontsize=50)
    ax1.set_ylabel(r'$(bs)$', fontsize=50)
    ax1.set_title(f'n = {n}', fontsize=60)
    ax1.view_init(elev=45)

    # Plot gamma* values on a 3D surface plot
    ax2 = fig.add_subplot(2, len(n_values), len(n_values) + i, projection='3d')
    surf_gamma_1 = ax2.plot_surface(xi, yi, zig, cmap='inferno',␣
↪edgecolor='none')
    ax2.plot_surface(xi, yi, np.where(mask_combined, zig, np.nan),␣
↪cmap='Greys', edgecolor='none', zorder=1)
    ax2.plot_wireframe(xi, yi, np.where(mask_combined, zig, np.nan),␣
↪color='black', alpha=0.7)
    ax2.set_xlabel(r'$(v)$', fontsize=50)
    ax2.set_ylabel(r'$(bs)$', fontsize=50)
    ax2.view_init(elev=45)

# Adjust layout to ensure clear visibility
plt.tight_layout()

# Display the plot
plt.show()
```